Biofouling Control Through Non-Toxic Means: Application of Zosteric Acid to Water Treatment Systems

Final Report of a Phase I Research Program

Submitted to:

National Water Research Institute
10500 Ellis Ave
Fountain Valley, CA 92728-0865

by

Richard C. Zimmerman, Project Coordinator and Principal Investigator
Moss Landing Marine Laboratories
P.O. Box 450
Moss Landing, CA 95309

David C. White, Principal Investigator
Center For Environmental Biotechnology
University of Tennessee
Knoxville, TN

Gill Geesey, Principal Investigator
Center for Biofilm Engineering
Montana State University
Bozeman, MT 59717-3980

Harry F. Ridgeway, Principal Investigator
Orange County Water District
10500 Ellis Ave.
Fountain Valley, CA 92728-8300

Robert Riley, Principal Investigator
Separation Systems Technology, Inc.
4901 Morena Blvd. Bldg. 809
San Diego 92117

16 July 1998

TABLE OF CONTENTS

I. Executive Summary

Zosteric acid (ZA), a natural product first isolated from the seagrass *Zostera marina*, significantly reduces the rate of biofouling accumulation by marine bacteria, algal spores and invertebrate larvae via a non-toxic mechanism that appears to interfere with the initial steps of adhesion. In early efforts, R. Zimmerman and J. Todd developed a direct synthesis of this compound in the laboratory, providing a route to industrial-scale production without exploiting sensitive natural populations. Developing ZA as an effective biofilm-control agent for water treatment systems, however, requires further research into its mechanism of action, its dose-effectiveness and its chemical compatibility with coating formulations and reverse osmosis (R/O) membranes. In this Phase I effort, experiments were performed to evaluate the interaction between ZA and R/O membrane systems, the leachability of ZA from foul-release silicone coatings and to test the breadth of ZA's effectiveness in controlling biofilm formation using a variety of bacterial strains and natural microbial populations in seawater and freshwater environments. Finally, the structure-function relationship underlying the biological mechanism of action were investigated using two structural analogs.

Aqueous ZA had no negative impact on water flux or salt rejection properties of cellulose acetate and FT-30 composite R/O membranes. Covalent linkage of ZA to polyamide membranes was attempted but analysis of the infrared ATR spectra suggest that some of the chemistry may not have occurred as expected. More work is required to validate the products from each step of the reaction scheme. Although aqueous ZA had no negative impact on membrane performance, it adsorbed irreversibly to polystyrene (PS) and cellulose acetate (CA) surfaces, decreasing their hydrophobicity. ATR/FT-IR analysis revealed persistent ZA signatures on these surfaces after several washes with clean water. ZA adsorbed reversibly to poly-octadecylmethacrylate (POMA), resulting in no change in its surface properties.

Incorporation of ZA into an RTV-11 silicone coating was attempted because (i) this polymer exhibits excellent foul-release properties in the absence of biologically-active agents and (ii) the polymer hydrates upon immersion, providing a means for mobilizing the water-soluble ZA salt dispersed within the coating. Uniform dispersal was achieved by moistening the ZA powder with methanol prior to its incorporation into the unpolymerized RTV-11. ZA had no effect on the dibutyl tin dilaurate-catalyzed polymerization of the silicone. Release rates of the uniformly-dispersed ZA were extremely high. Coatings prepared with 5 and 10 wt% ZA were depleted in 48 h exposure to running seawater while 25 wt% coatings maintained high release for the entire 7 d exposure.

ZA-impregnated silicone coatings performed well against marine biofilms as long ZA was leaching from the surface. Depleted coatings containing residual levels of unreleased ZA accumulated a higher biofilm load than pure silicone controls. This enhancement of biofilm adhesion by immobilized ZA was also observed in laboratory experiments. Pre-exposure of *Pseudomonas aeruginosa* to ZA enhanced cell attachment to PS surfaces in laboratory tests, while incorporation of leachable ZA into the PS film produced a slight reduction in bacterial attachment. Similarly, *Mycobacterium* strain BT12-100 accumulated to higher densities on CA membranes containing irreversibly adsorbed ZA than on untreated CA membranes. Immunolocalization studies using *Shewanella putrefaciens* revealed staining of the exopolymeric

regions between the agglutinated cells while boundaries between dividing cells remained free of immuno gold.

Two analogs of ZA (4-pentylphenyl acid sulfate and octyl sulfate) were found to possess significant antimicrobial activity not shown by ZA itself. In addition, 4-pentylphenyl acid sulfate (4-PPAS) incorporated into an RTV-11 silicone polymer coating was more effective than native ZA in preventing biofilm formation by *Vibrio harveyi* in flowcell tests. Octyl sulfate was not available in sufficient quantity for flowcell tests in this Phase I effort. Thus, modifications of the basic chemical structure of ZA may dramatically improve the biofilm control properties of these sulfated phenolic acids.

The heparin-like activity of ZA shown in early work by R. Zimmerman prompted an investigation into the feasibility of polymerizing ZA as a method of increasing specific activity against fouling organisms. Co-polymerization with acrylamide appeared successful, as the reaction mix showed a significant increase in viscosity. Unfortunately here was insufficient material synthesized for biological testing in this Phase I effort.

The experiments performed in this Phase I effort have demonstrated that:

- ZA is chemically compatible with polymers used for foul-release coatings and R/O membranes used in water treatment applications,
- Effective biofilm control requires ZA be freely dissolved in the aqueous medium,
- Immobilizing ZA on membrane surfaces enhances biofilm adhesion,
- Target-specificity shows significant variability among microbial strains,
- Analogs of ZA possess strong activity against ZA-resistant bacterial strains, increasing the potential range of environmentally-friendly molecules available for biofilm control,
- Different formulations and delivery systems may be required to successfully exploit the non-toxic surface-binding mode-of-action exhibited here to control biofilm formation in water treatment applications,

Further experiments into the non-toxic mechanism illustrated by ZA should prove fruitful in the search for effective and affordable non-polluting technologies for biofilm control in water treatment applications.

II. General Introduction

Nature has evolved a variety of strategies to prevent or minimize fouling of natural surfaces in aquatic environments. Organisms use physical means, including the sloughing of the outer tissue layer (Patton 1972, Rublee et al. 1980, Filion-Mykelust and Norton 1981), the generation of external surfaces that minimize bioadhesion (Milne and Callow 1985), and the production of secondary metabolites that can deter potential fouling organisms and predators.

The secondary metabolites employed as defensive agents are as diverse as the organisms manufacturing them. Those known agents include elemental vanadium, inorganic acids and a wide variety of organic components including saponins, terpenoids and phenolic acids (Davis et al. 1989). We isolated a novel sulfated phenolic acid from the marine angiosperm *Zostera marina* L. (eelgrass) that possesses significant antifouling activity against aquatic organisms including bacteria, algal spores and invertebrate larvae (Todd et al. 1993, Zimmerman et al. 1995). The compound, p-sulfooxy cinnamic acid (common name: zosteric acid or ZA), is hydrophilic and readily hydrolyzed under acid conditions which may be why it was not isolated previously. ZA contains no metal or halogen components that are likely to accumulate to toxic levels in the environment, and the half-life of this compound in raw seawater is about 12 d. Unlike many of the naturally occurring terpenoids showing antifouling activity, the structural simplicity of zosteric acid allows for complete laboratory synthesis of the native compound, eliminating the need to exploit natural populations of eelgrass for this material or to limit synthesis to small portions of the molecule.

The broad-spectrum effectiveness of zosteric acid is based on a proposed non-toxic mechanism of action involving the sulfate-mediated binding of cells to surfaces. In solution, zosteric acid appears to mediate the first stage of attachment between the cell and another surface. When bound to ZA dissolved in the aqueous medium, the ability of cells to attach to host surfaces is altered. A simple wash with fresh seawater restores full biological function of the exposed cells. Thus, ZA is not acutely toxic to the targeted biofouling organisms. ZA can affect other sulfate-mediated interactions between cells including sperm-egg fusion, red blood cell agglutination, and human prothrombin (PT and APTT) clotting times (Zimmerman, unpubl.). The performance of ZA suggests that it acts generally on sulfate or heparin-binding domains of proteins, polysaccharides and glycoproteins, many of which represent surface adhesins necessary for mediating cell-surface and cell-cell adhesion. Although ZA performs much like heparin sulfate in some applications, there are significant quantitative differences. Monomeric ZA is approximately 10-fold more effective than heparin at blocking sperm-egg fusion and red blood cell agglutination but is much less effective than heparin in prolonging human PT and APTT clotting times. Free inorganic sulfate, in contrast, has no measurable effect on cell-surface interactions even though it is present at high concentration in many aquatic environments, including seawater ($[SO_4^{=}] = 28$ mM). The unsulfated analog of ZA, p-coumaric acid, shows minimal antifouling activity and has no anticoagulant properties (Todd et al. 1993; Zimmerman unpubl.). Thus, simple changes in the organic structure of the molecule may significantly modify the performance of a sulfated agent such as ZA.

Small scale experiments were conducted to understand how ZA interacts with biofilm-forming organisms and with the target surface as a prelude to further exploration of the non-

polluting model for biofilm control in water treatment applications. The experiments described below represent a Phase I investigation into the antifouling properties and structure-function relationships of ZA and two analogs. The results provide initial evaluation of the potential for this non-toxic approach to control biofilm formation in water treatment and distribution applications.

III. PHASE I OBJECTIVES

Experiments conducted under this Phase I study sought to quantify the effectiveness of ZA and derivatives as biofilm control agents, and to learn more about the mode-of-action of ZA that will help in designing practical solutions for biofilm control based on non-toxic approaches. Overall objectives were to:

1) Test effectiveness of ZA and ZA derivatives in bulk solution and various coatings for quantitative antifouling activity (AF) as a model for non-polluting, biodegradable bioactive compounds,

2) Test the interaction of ZA with inert polymer surfaces and R/O membranes with regard to adsorption, desorption, solubility and membrane function,

3) Explore the non-toxic mechanism-of-action of ZA with bulk-phase bacteria in liquid culture and in the presence of settling surfaces and R/O membranes.

IV. INVESTIGATOR REPORTS

A. Biological Activity of Zosteric Acid and Derivatives

R. Zimmerman
Moss Landing Marine Labs, P.O. Box 450, Moss Landing, CA 9039

1. Objectives

This component of the study had six objectives:

1) Synthesize zosteric acid and derivatives for experimental use by the research team,
2) Investigate the potential for polymerization of ZA into oligomeric (10-20mer) units,
3) Prepare coated coupons containing ZA and derivatives for experimental evaluation by the research team,
4) Evaluate the effects of ZA and analogs on bacterial growth in liquid culture,
5) Evaluate release rates and antifouling properties of the prepared coatings in seawater,
6) Explore the surface-binding mechanism of ZA responsible for mediating cell-surface interactions.

2. Methods and Materials

Synthesis of Zosteric Acid and Analogs

The sodium salt of zosteric acid was prepared according to the sulfonation reaction described by Todd et al (1993) and purified by recrystallization. Final purity was greater than 99% as determined by mass spectrometry, NMR and elemental analysis. Aliquots were distributed to the research team for independent analyses in various assays. See Sections **IV.B** to **IV.E** of this report for detailed results.

Two derivatives were tested along with ZA to determine the structural features responsible for antifouling activity. Previous work (Todd et al. 1993; Zimmerman unpubl.) showed the antifouling activity was critically dependent on the presence of a sulfate moiety. This study evaluated the effects of structural changes in the unsulfated hydrocarbon tail and aromatic ring on biological activity. 4-Pentylphenol acid sulfate (4-PPAS) was synthesized to test the effect of converting the carboxyvinyl functionality on the original ZA molecule into a simple 5-C alkane structure (Fig. 1) using the procedure of Ragan (1978). The product was isolated in 33% yield after recrystallization from methanol when using a reaction temperature of 35 – 40° C. Octyl sulfate, a surfactant used in polymerization control processes, was purchased from Aldrich Chemical Co. to evaluate the antifouling significance of replacing both the aromatic and carboxyvinyl groups with an 8-C alkane tail.

Linear polymerization of ZA: acrylamide was explored at molar ratios of 1:2, 1:4 and 1:8. Polymerization was initiated using the hydrochloride salt of 2,2'-azobis(2-aminopropane) at 80° C. Linear polymerization was assured by the absence of cross-linking agents, such as bis-

acrylamide, from the reaction mixture.

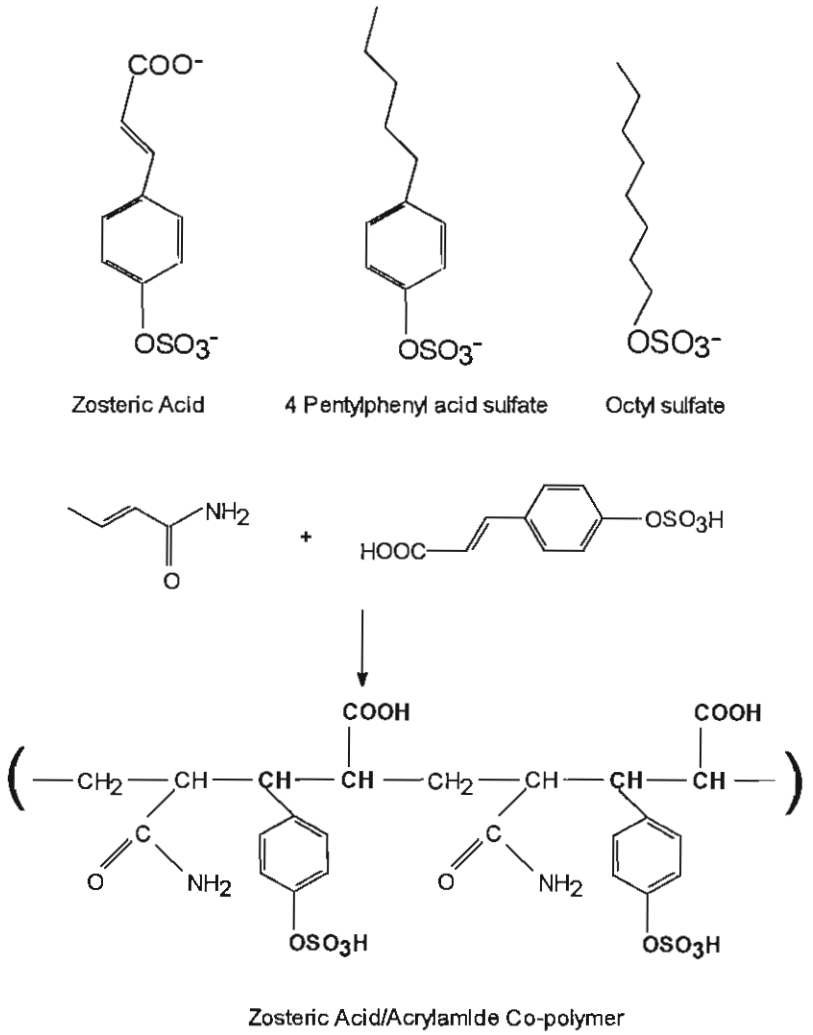

Figure 1. Chemical structures of zosteric acid, 4-pentylphenyl acid sulfate, octyl sulfate and ZA/acrylamide co-polymer.

Preparation of Coatings

Only ZA and 4-PPAS were available in sufficient quantity for incorporation into silicone coatings. Coatings for steel and glass coupons were prepared by mixing ZA with RTV-11 silicone paint obtained from General Electric Corp. Dry ZA powder does not disperse well in hydrophobic RTV-11, and such neat loadings caused the agent to clump in the mixture, producing coatings with rough surfaces. Moistening the ZA powder into a thick paste with 100% methanol, however, produced more uniform dispersion and smoother coating surface when dry. Coatings were prepared using the ZA-methanol paste at various loadings from 5 to 25 wt% and applied to primed glass microscope slides by spin-coating in a tabletop centrifuge. The mass of dry coating applied to each slide was determined gravimetrically. Three coupons loaded with 25 wt% of 4-PPAS in RTV-11 were prepared as for ZA and sent to D.C. White for analysis

of biofilm formation in flowcell studies (see Sec. **IV.B.** for details).

RTV-11 Coatings: Zosteric Acid Release Rates and Biofilm Accumulation

ZA release rates from the slides coated with 5, 10 and 25 wt% ZA in RTV-11 were measured in stirred glass beakers filled with measured volumes of seawater. Water samples were removed at regular intervals and ZA concentration determined by spectrophotometric absorption at 274 nm standardized to known concentrations of fresh ZA dissolved in seawater. Release rates were calculated from the slope of [ZA] vs. time for each coupon. After measuring initial release from freshly-prepared coatings (Day 1), slides were placed in a 1 m^3 tank of flowing seawater. Subsequent release rate measurements were performed on Days 2, 3 and 7.

Accumulation of the developing microalgal biofilm on silicone-coated glass slides was quantified optically using an integrating sphere spectrophotometer capable of accurately measuring absorbance of turbid samples. Pre-exposure absorption spectra of each slide were measured and subtracted from subsequent spectra measured on days 2, 3 and 7. The 440 nm absorbance peak (due primarily to chlorophyll) was used as an index of biofilm density.

Microbial Growth and Agglutination Assays

Antimicrobial properties of ZA, 4-PPAS and octyl sulfate were investigated using log-phase cultures of the marine bacteria *Vibrio harveyi* and *Shewanella putrefaciens*. Cells were grown in complete seawater medium (seawater + yeast extract + bacto tryptone) liquid cultures containing candidate agents at a range of concentrations up to 20 mM. Growth and agglutination of each culture was monitored spectrophotometrically (OD_{600}).

3. Results and Discussion

Polymerization of Zosteric Acid

Reactions performed at 1:4 and 1:8 molar ratios of ZA:acrylamide showed an increase in viscosity, indicating successful co-polymerization of ZA and acrylamide. Sulfur elemental analysis of the polymers indicated 42% incorporation of ZA. Due to the small reaction size of this pilot effort, there was insufficient material for evaluation of polymer length or biological activity. Larger-scale synthesis will allow us to perform size exclusion chromatography, NMR spectroscopy, and bioassays on the different linear polymers formed. Copolymers of ZA with 2-hydroxyethyl acrylate, maleic anhydride and p-styrenesulfonic acid should also be investigated. The reaction pathway and probable polymer structure of the ZA-acrylamide co-polymer is illustrated in Fig. 1.

Coating Preparations and Zosteric Acid Release Rates

Moistening the ZA with methanol dramatically improved dispersal of the agent in RTV-11. Neither the presence of ZA or the methanol wetting agent appeared to affect the RTV-11 cure process or coating integrity. Resulting coating surfaces were smooth and free of visible

surface roughness at loadings up to 15 wt%. ZA concentrations above 15% produced increasingly rough and grainy surfaces, but polymer integrity appeared intact.

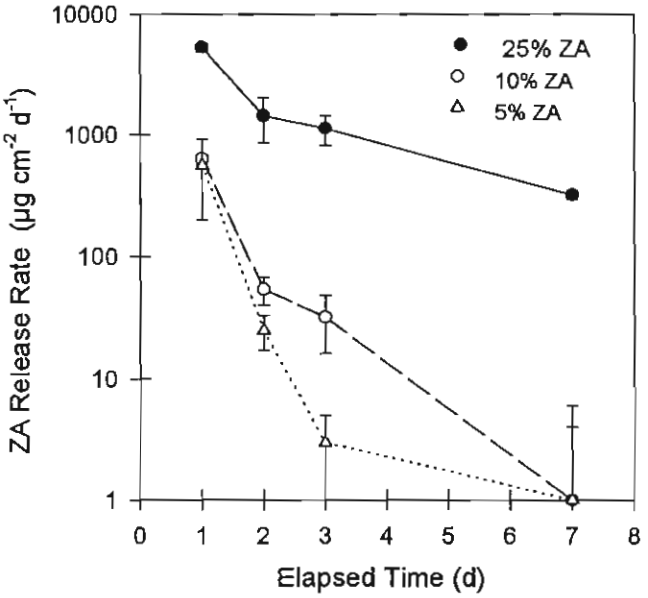

Figure 2. Rates of zosteric acid release from impregnated RTV-11 silicone coatings.

Initial release rates of ZA from the freshly prepared coupons exceeded 10 mg cm^{-2} d^{-1} prior to seawater exposure and declined as a second order (exponential) function of time incubated in seawater over the next seven days (Fig. 2). These extremely high rates represent the release of approximately 75% of the total ZA loaded into the 25 wt% coupons within 48 h. Release rates of slides coated with 5 and 10 wt% ZA loadings dropped to 2 µg cm^{-2} d^{-1} after 24 h, and no ZA release was detected after 48 h. Release rates of coupons coated with 25 wt% ZA loading also decreased dramatically over time, but remained above 100 µg cm^{-2} d^{-1} for the 7-day duration of this exposure. Integrated loss of ZA calculated by fitting an exponential decay curve to the release rate data revealed that the 5 and 10 wt% coatings released only 26 and 16% of their originally loaded ZA (Table 1). About 84% of the originally loaded ZA was released from the 25 wt% coatings. Residual ZA content of all coatings estimated by these calculations at the end of the incubation were remarkably constant, and ranged from 0.5 to 1.37 mg cm^{-2}. This relatively constant residue and may represent an immobilized reservoir within the coating that does not release.

Table 1. Mass balance calculations based on measured rates of ZA release from impregnated silicone coupons after 7 days immersion in seawater.

ZA Loading (WT%)	Integrated Loss (mg cm^{-2})	% of Total ZA Released	% of Total ZA Remaining	Residual ZA (mg/cm2)
5	0.180	26.4	73.6	0.50
10	0.264	16.2	83.8	1.37
25	4.881	88.7	11.3	0.62

The degree of coating hydration after 7 days in seawater increased dramatically the

presence of ZA (Fig. 3). Control coupons (no ZA) contained about 10% water by weight and the degree of hydration increased to about 60 wt% at all ZA loadings. This large accumulation of water by coatings loaded with as little as 5 wt% ZA indicates that rapid leaching of ZA results from coating hydration, as ZA cannot migrate through the coating unless dissolved in water. It also indicates that extremely low release rates from the 5 and 10 wt% coatings did not result from poor hydration. The 110% hydration value of one of the 10% coupons probably represents

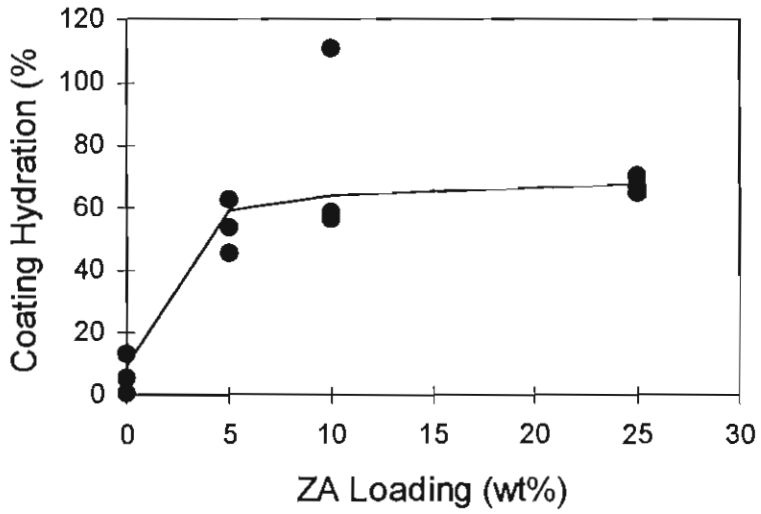

a measurement error.

Figure 3. Coating hydration state after 7 d immersion in seawater, plotted as a function of original ZA content .

Biofilm Growth on ZA-Impregnated Coatings

Coating effectiveness against biofilm formation was clearly related to ZA release rates. Density of the microalgal biofilm, as measured by A_{440}, increased in a second-order (exponential) fashion on the Blank, 5 and 10 wt% ZA coatings (Fig. 4). The 25 wt% coatings,

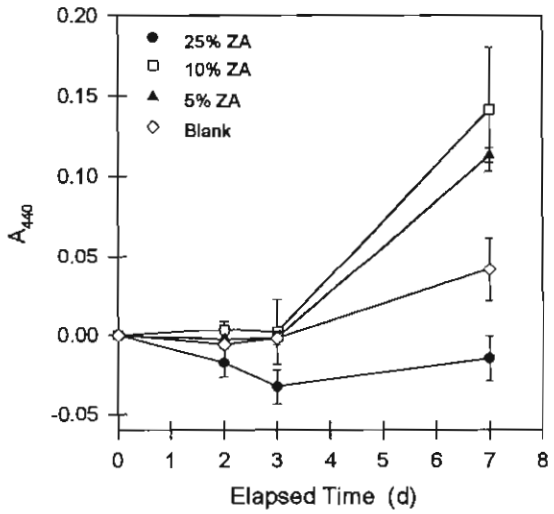

Figure 4. Marine biofilm density on ZA-impregnated silicone coatings during a 7-d incubation in running seawater.

however, remained free of measurable algal biofilm for the duration of the 7 day experiment. Not only were release rates from the 5 and 10 wt% coatings too low to prevent biofilm development, these coatings actually developed significantly higher biofilm loads than the Blank (0 wt%) coating. Thus, residual levels of ZA immobilized within the coating may have promoted microalgal adhesion to the coating surface, as was shown for sulfated PS surfaces (Sec. **IV.C**) and CA membranes (Sec. **IV.D**). Regardless, these data clearly demonstrated that ZA can prevent marine biofilm formation at release rates above 10 $\mu g\ cm^{-2}\ d^{-1}$. An improved method for slowing the initial release will be required before ZA-impregnated silicone coatings will be practical.

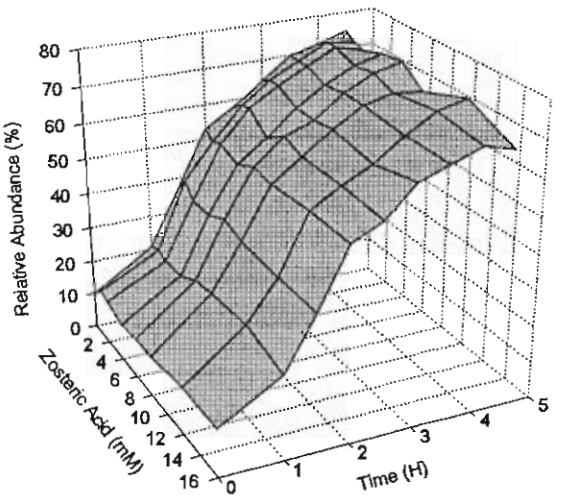

Figure 5. Growth of *Vibrio harveyi* on complete marine medium and a range of zosteric acid concentrations.

Microbial Growth and Agglutination Assays

Although ZA shows promising biofilm control properties when incorporated into leachable coatings such as RTV-11 silicone, it did not prevent growth of marine bacteria such as *Shewanella putrefaciens* and *Vibrio harveyi* in liquid culture at concentrations up to 16 mM. ZA had no measurable effect on the growth dynamics of *V. harveyi* (Fig. 5), but it caused significant agglutination of *S. putrefaciens* in a concentration dependent fashion that was visible to the naked eye. This was manifest in the optical density data as an apparent decrease in relative abundance (Fig. 6a). There was no difference, however, in cell abundance of stationary phase culture density at 5 h, based on direct counts. Immuno-gold labeling of *S. putrefaciens* aggregations with a polyclonal antiserum raised against ZA showed distinct staining at the aggregated cell junctions (Fig. 6b). Chains of dividing cells, in contrast, showed no significant labeling at their junctions. This indicates that ZA promotes agglutination of some bacteria through a surface-binding mechanism.

In contrast to ZA, 4-PPAS effectively inhibited growth of *V. harveyi* in liquid culture at concentrations above 2 mM (Fig. 7) but the onset of growth inhibition showed a significant lag effect. Even in the presence of high concentrations of 4-PPAS, growth rates appeared normal for about 2 h. The dramatic crash of growing cultures after 3 h suggests that 4-PPAS may be converted by the culture into a 2° metabolite with toxic properties. The growth-inhibiting capacity of 4-PPAS, furthermore, remains consistent with the strong antifouling capacity of this material when incorporated into a silicone coating (see Sec. **IV. B.**). Thus, modification of the

carboxyvinyl tail of ZA into a saturated alkane moiety converts the metabolically benign ZA molecule into an agent with significant antibacterial potential. Clearly, additional work is warranted on the antifouling properties of 4-PPAS.

Octyl sulfate, like 4-PPAS, exerted a significant effect on growth of V. harveyi in liquid culture. This material, however, exhibited a more typical toxic effect that increased with concentration. There was no apparent lag in the toxic effect, as had been observed with 4-PPAS,

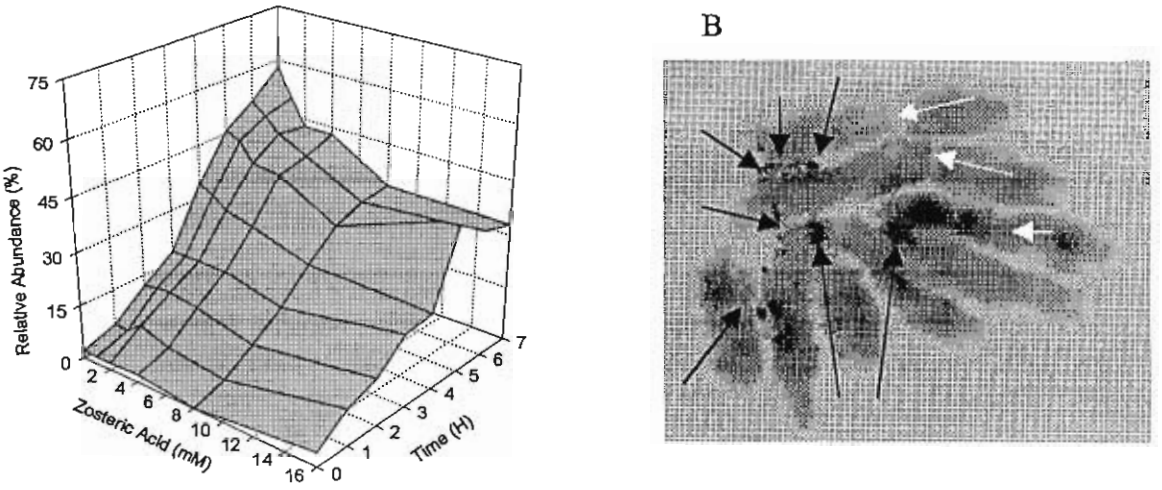

Figure 6. A. Growth curve of *Shewanella putrefaciens* in complete marine medium and a range of zosteric acid concentrations. **B.** Electron micrograph of an *S. putrefaciens* aggregation shows positive immuno-gold labeling of ZA-binding regions on cell surfaces (black arrows) and unlabeled boundaries between dividing cells(white arrows).

and bacterial growth was prevented completely at concentrations above 3 mM (Fig. 8). Octyl sulfate was prone to foaming in solution and this agent may act as an ionic detergent in solution. It, too, deserves further exploration as a potential biofilm control agent.

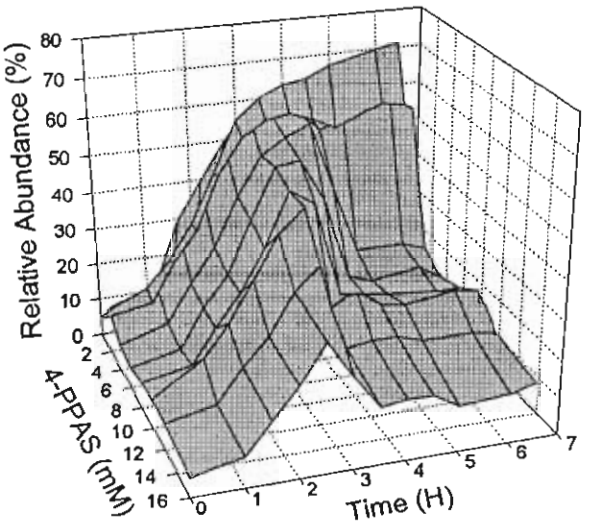

Figure 7. Growth of *Vibrio harveyi* in complete marine medium and a range of 4-pentylphenyl acid sulfate concentrations.

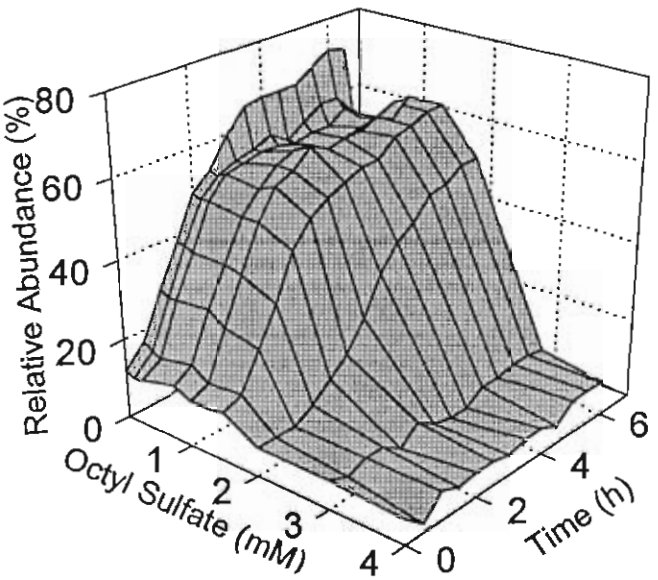

Figure 8. Growth of *Vibrio harveyi* in complete marine medium and a range of octyl sulfate concentrations.

4. Conclusions

The biological studies performed here support the surface-binding mode-of-action for ZA. By binding to cell surfaces, ZA can mediate cell adhesion to inert materials and other cells. In the case of cell agglutination, ZA appears to form a bridge causing cells to agglutinate that otherwise would remain free. Freely-released ZA appears to inhibit formation of biofilms on silicone coatings, but residual ZA tethered to the coating surface may actually promote biofilm adhesion. Two new analogs of ZA (4-phenylpentyl acid sulfate and octyl sulfate) showed significant antifouling activity were tested, and their ability to prevent biofilm formation should be explored more extensively. The synthesis of polymeric ZA also appears possible. Given the heparin-like binding properties of ZA, polymerization may be an important strategy for strategic targeting to specific cell systems and organisms.

5. References

B. Attachment of cells and biofouling of surfaces in the presence of Zosteric Acid

M. S. Zinn[1], R. D. Kirkegaard[1], and D. C. White[1,2]

[1]Center for Environmental Biotechnology, University of Tennessee, Knoxville, TN 37932
[2]Environmental Sciences Division, Oak Ridge National Laboratory, Oak Ridge, TN 37831

1. Objectives

During the reporting period, experiments were performed in order to investigate the influence of zosteric acid (p-coumaric acid sulphate, ZA) on bacteria in sea and drinking water systems.

The following objectives were of interest:

1) Influence of ZA on the growth of bacteria in submerged cultures,
2) Verify the attachment of cells on surfaces in presence of dissolved ZA,
3) Test antifoulant efficiency of coated silicone-ZA metal coupons in a laminar flowcell.

In the following different organisms were used under special test conditions.

2. Material and Methods

Test organisms

Vibrio harveyi (ATCC 14126) was used as a test organism in sea water systems. *Escherichia coli* M182 (gift from Dr. A. Goodman, Flinders University, Australia) was used for drinking water experiments. The strain M182 harbors the gene for the green fluorescent protein GFP on an insert of the chromosome (mini-Tn10:gfp:kan).

Pseudomonas aeruginosa R5 (lab collection) is a mutant of *P. aeruginosa* O6 (ATCC 33353) and is not motile (lack of flagella), moreover R5 attaches to surfaces more efficient than the original strain O6.

Staphylococcus aureus (ATCC 6538) is an isolate of the drinking water system.

Maintenance and growth

V. harveyi was maintained on sea water complete medium (SWC) agar plates and sub-cultured every three weeks. One liter of SWC consists of 5 g l^{-1} bacto-tryptone, 3 g yeast extract, 3.75 glycerol, 750 ml filtered sea water, and 250 ml distilled water. The medium was heat sterilized and for agar plates 15 g agar was added. For the chemostat and flowcell experiments the strain was cultured in artificial sea water (ASW) medium supplemented with 0.01% glycerol, 0.02% casamino acids, and 10 mM TRIS buffer (pH 7.5).

E. coli, *P. aeruginosa*, and *S. aureus* were maintained on Luria broth (LB) agar plates and transferred to new plates monthly.

For growth and attachment studies the minimal medium E2 (Lageveen et al., 1988) was used, containing (per liter):

3.5 g $NaNH_4HPO_4*4H_2O$, 7.5 g $K_2HPO_4*3H_2O$, 3.7 g KH_2PO_4. The trace elements were stored in three stock solutions and added separately: 1 ml of 1 M $MgSO_4*7H_2O$, 1 ml of 0.01 M $FeSO_4*7H_2O$ in 1 N HCl, and 1 ml of MT stock solution that contained (per liter 1 M HCl): 1.98 g $MnCl_2*4H_2O$, 2.81 g $CoSO_4*7H_2O$, 1.47 g $CaCl_2*2H_2O$, 0.17 g $CuCl_2*2H_2O$, and 0.29 g $ZnSO_4*7H_2O$. For growth studies, medium E2 was supplemented with D-glucose and the pH was adjusted to 7.1 using 5N KOH. In general, the medium was filter sterilized.

The growth temperatures were: room temperature for *V. harveyi*, 37□C for *E. coli*, and 25□C for *P. aeruginosa* and *S. aureus*.

Culture vessels

Batch cultures were performed in 500 ml shake flasks containing 150 ml medium. Generally, the inoculum of batch cultures was 5-10% of the culture volume. The culture broth was mixed using magnetic stir bars.

Continuous cultures were carried out in home made 2 liter bioreactors with a culture volume of 1.3 liter. The volume was kept constant by an overflow device. The cultures were aerated at 0.7 vvm with filter-sterilized air and its dispersion was supported by a stir bar turning at 300 rpm.

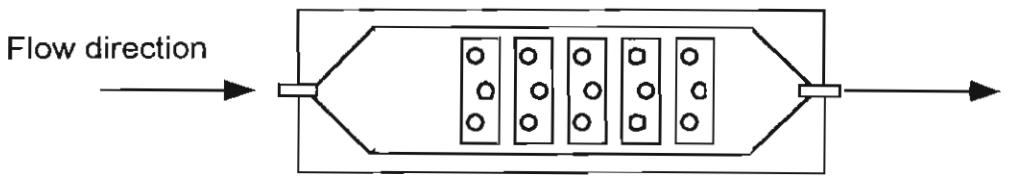

Figure 1. Schema of a flowcell which is used to investigate the attachment of cells and the effect of antifoulants. The rectangles represent test coupons and the circles indicate sample ports for tryptophan and bioluminescence readings.

Flowcells (Fig. 1) were used to study attachment and biofouling on surfaces in a laminar stream of liquid (Mittelman et al., 1993). The flowcell measures 150 mm x 285 mm with a flow channel of 2 mm in depth. The working volume was 75 ml. In the bottom half of the channel 5 polished stainless steel coupons (35 x 70 x 3 mm, Metal Samples, Munford, AL) were inserted flush with the flow channel. These coupons were also the test bed for silicone coatings. Hollow, polypropylene screws with a glass window towards the liquid stream are placed in the upper half of the flow channel. Thus, fluorescence and light measurements of each coupon could be performed (3 screws per coupon). A peristaltic pump (Watson Marlow) upstream of the flowcell pumped medium or culture broth from a chemostat into the flowcell. Coated coupons were

primed in the flowcell for two days with sterile medium. At the end of the experiment the flowcell is taken apart, and the cells on the coupons were collected in 10 mM phosphate buffer (pH 7.0) using probe sonication.

Mini-flowcells (Fig. 2) (Palmer and Caldwell, 1995) were used for the study and documentation of attachment of cells and biofilm growth on glass. Each mini-flowcell has two flow chambers containing a volume of 200 µl each. They are covered by two microscope coverslips sealed by silicone rubber (RTV 118, General Electric Co.). Downstream of the mini-flowcell a peristaltic pump (Watson Marlow 205S) was installed to attain a pulse free laminar flow. For the investigation of the biofilm under the microscope, the mini-flowcell was washed with sterile sea water or isotonic saline at the same pumping rate for 5 minutes. Then, the liquid flow was stopped and the mini-flowcell disconnected from feed and outlet tubing. Due to the design of the cell no liquid could escape from the flow chamber while the examination under the microscope.

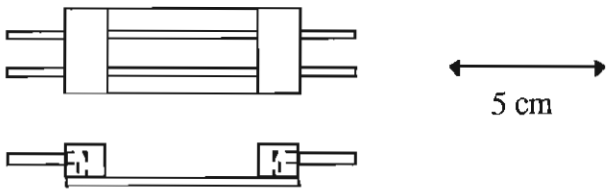

Figure 2. Mini-flow cell to study biofilms under the microscope (above: top-view; below: cross-section).

Determination of the biomass

Optical density

The optical density of batch and chemostat cultures was measured with a spectrophotometer (Shimadzu UV-120-01, Japan) at a wavelength of 660 nm (*V. harveyi*) and 600 nm (*E. coli, P. aeruginosa,* and *S. aureus*) against 0.9% NaCl in water (isotonic saline). Appropriate dilutions of the samples were performed with sterile sea water (*V. harveyi*) or isotonic saline (*E. coli, P. aeruginosa,* and *S. aureus*), such that the optical density was below 0.4.

Acridine orange counts

Cell samples were diluted 1 : 10 in either ASW or 10 mM phosphate buffer. 1 to 2 ml were filtered (0.2 µm pore size, black polycarbonate membrane, Poretics Corp., Livermore, CA) and subsequently stained with an acridine orange solution (1.0 mg ml^{-1} acridine orange in 100 mM phosphate buffer, pH 7.5) during 3 minutes. The filters were air dried and mounted on microscope slides. Under epifluorescence (UV light) the cells appeared orange and could be differentiated from the background.

Viable cell counts

The same sample for the acridine orange counts was used for the determination of the viable cell number (only for *E. coli, P. aeruginosa,* and *S. aureus*). 100 µl of the sample and dilutions of it (10x and 100x in isotonic saline) were distributed on LB agar plates. After 24 hours the cell number was determined by the number of visible colonies.

Fluorescence of cells

The tryptophan fluorescence of cells was measured with a F212 Fluorolog II fluorometer (Spex Industries Inc., Edison, NJ) at 295 nm excitation and 342 nm emission wavelength (Arrage et al., 1995). Excitation and emission scans revealed a light quenching effect of tryptophan fluorescence caused by zosteric acid. This effect could be avoided by the use of the GFP containing *E. coli* (Arrage and White, 1997; Palmer et al., 1997). At an excitation of 467 nm and an emission of 509 nm the interference with ZA was significantly reduced (Fig. 3).

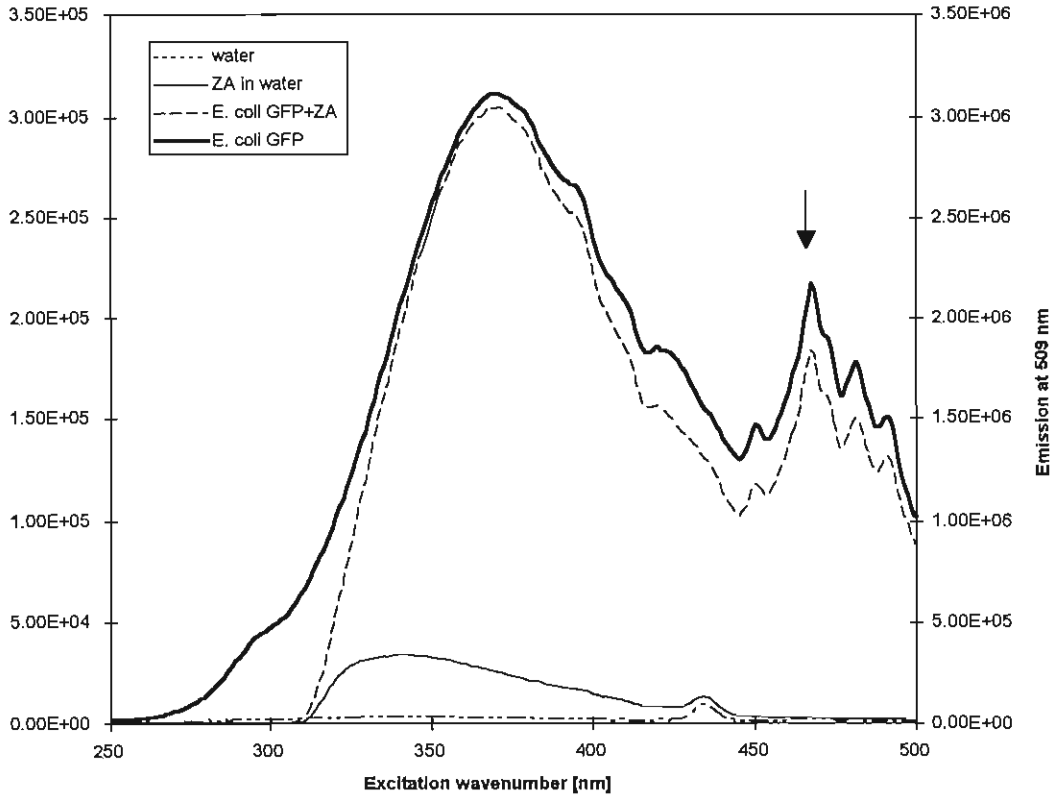

Figure 3. Determination of the excitation wavenumber for GFP containing *E. coli* M182 and the interference of the emission signal with ZA at 509 nm emission. The excitation wavenumber of 467 nm (arrow) was chosen to measure the GFP signal in presence of ZA.

Bioluminescence of V. harveyi

The bioluminescence of *V. harveyi* in biofilms is a biomass indicator on condition that the cell physiology is not changed (bioluminescence is related to the activity of the cell metabolism)

(Hastings and Nealson, 1981). The bioluminescence was measured with an Oriel liquid light pipe-photomultiplier tube-ammeter light system (Oriel Corp., Stratford, CT). The measurements were performed in a light protecting bag to ensure no interference with external light.

Cell counts on glass surfaces

The number of attached cells to the glass cover slide of mini-flowcells was determined by the evaluation of pictures taken by a CCD video camera (Hamamatsu photonics K.K. C5810, Sunayama-Cho, Japan), mounted on a microscope (Leica DMBR, Wetzlar, Germany). The digital pictures were saved as Adobe Photoshop files (Adobe systems, Mountain View, CA) and further processed (particle size, area coverage) with the software Ultimage (GTFS, Santa Rosa, CA). A picture of a grid of 0.01 mm was used to calibrate Ultimage.

Microscopy

Confocal laser microscopy images were obtained using a Leitz laser imaging system, which was coupled to a microscope (Leica DMBR, Wetzlar, Germany). Biofilms of the mini-flowcells were studied using 100 X oil immersion lenses.

The same microscope equipped with a CCD video camera (Hamamatsu photonics K.K. C5810, Sunayama-Cho, Japan) was used for the investigation of the biofilm structure on metal coupons. During the observation the coupons were kept in isotonic saline in a basin. Two lenses were used: 10 X (through air-water interface) and 60 X (water immersion objective).

3. Results and Discussion

Growth of submerged cultures in presence of ZA

Batch cultures of Vibrio harveyi

V. harveyi was cultured at 24°C in five 500 ml shaking flasks containing sea water complete medium and different concentrations of ZA. The growth of biomass was described by the measurement of the optical density at 660 nm. Two log-phases with the specific growth rates (μ) shown in Table 1 could be determined.

Table 1. Specific growth rates of *V. harveyi* in shake flask cultures in supplemented ASW medium with different ZA concentrations.

Zosteric acid [mM]	$\mu 1$ [h^{-1}]	$\mu 2$ [h^{-1}]
0	0.27	0.12
0.001	0.25	0.11
0.010	0.25	0.12
0.100	0.23	0.12
1	0.23	0.13

The first one was ZA influenced (0 - 2 hours, 4 data points), whereas the second one was ZA independent (2 - 8.4 hours, 5 data points).

Interpretation: The interpretation of the data is difficult, as no microscopic investigations of the cell appearance were performed. The reduced growth rate ($\mu 1$) in presence of ZA could be explained either by cell agglutination (reduced optical density), or by the decreased uptake of energy rich nutrients.

Batch and chemostat cultures of E. coli

E. coli was grown in shake flasks containing medium E2 with 1.8 g glucose l^{-1} (Fig. 4). The growth curves showed that ZA cells grew slightly faster, however, the concentration of ZA did not change the specific growth rate of the cells nor is ZA a carbon source (Tab. 2).

Interestingly, the final optical densities of the cultures differed significantly (Fig. 4).

Table 2. Specific growth rates of shake flask cultures of *E. coli* in medium E2 with 1.8 g glucose l^{-1} and different concentrations of ZA.

Zosteric acid [mM]	**μ [h^{-1}]**
0	0.52
0.75	0.56
1	0.56
2.5	0.52
5	0.56
5 (no glucose)	<0.01

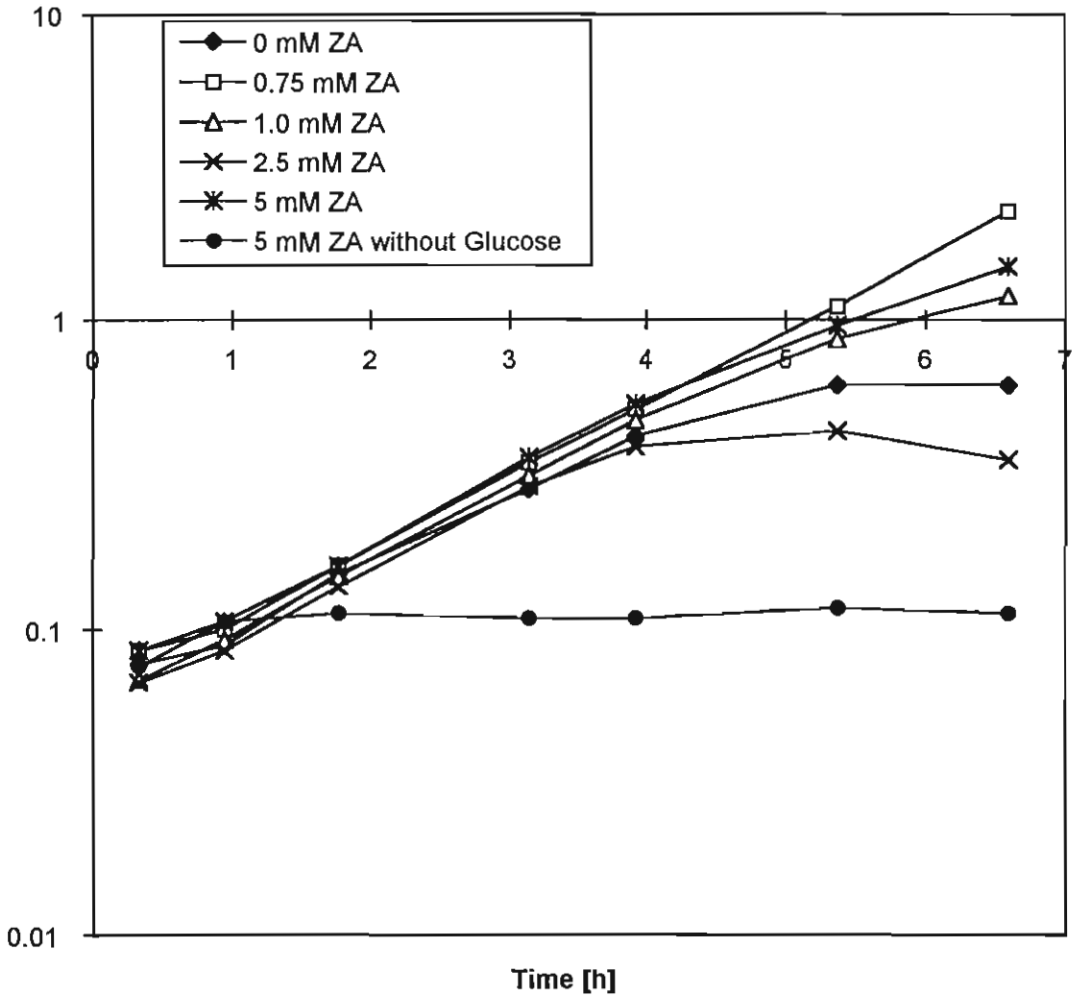

Figure 4. Batch cultures of *E. coli* in medium E2 with 2.0 g glucose l^{-1} in presence of different concentrations of ZA.

In another experiment *E. coli* was grown in two chemostat cultures on medium E2 with 0.18 g glucose l^{-1} at the same dilution rate of 0.25 h^{-1}. One culture was grown in presence of 5 mM ZA, the second was used as a control (0 mM ZA). The steady-state optical densities were significantly different: 2.04 with ZA and 1.37 without ZA, respectively.

Interpretations: ZA does not influence the growth rate of the cell, however, the yield of biomass is increased with higher ZA concentrations. ZA is not a carbon source for *E. coli*.

Batch of P. aeruginosa

P. aeruginosa was grown in two shake flasks in medium E2 containing 1.8 g glucose l^{-1} with or without 5 mM ZA, respectively (Fig. 5). The specific growth rate was almost identical for both cultures (0.43 h^{-1} with ZA and 0.42 h^{-1} without ZA). The cells of both cultures were

examined using microscope techniques (arrows in Figure 5 indicate the time points of the sample shown in Figure 6a and b).

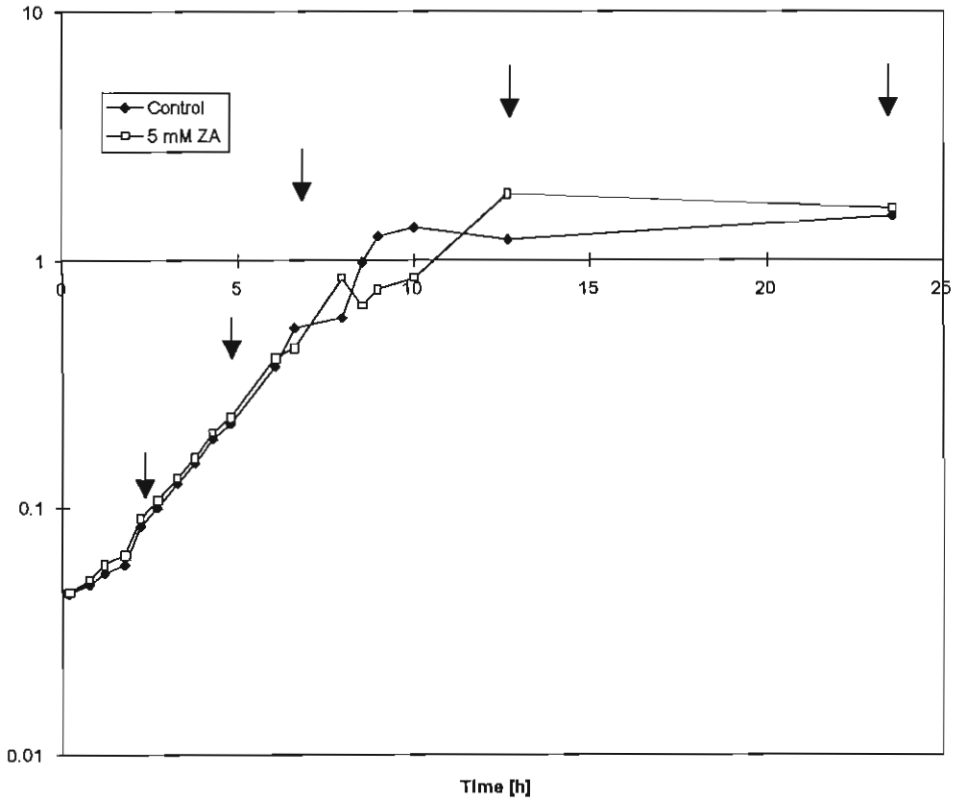

Figure 5. Growth of *P. aeruginosa* in shake flasks with medium E2 and 1.8 g glucose l^{-1}. Arrows indicate the samples that were examined under the microscope (Fig. 6a and 6b).

It can be seen that the cells without ZA agglomerate to piles during the exponential growth phase and get again separated in the stationary phase. The opposite effect could be observed in presence of 5 mM ZA. The cells in the exponential phase clumped less, however, in the stationary phase more cells were attached to each other.

Interpretation: The agglomeration of *P. aeruginosa* cells is reduced in presence of ZA in the exponential phase, whereas increased agglutination could be observed in the stationary phase.

Batch culture of S. aureus

S. aureus was grown in two shake flask cultures in medium E2 containing 1.8 g glucose l^{-1}. One culture was grown in presence of 5 mM ZA.

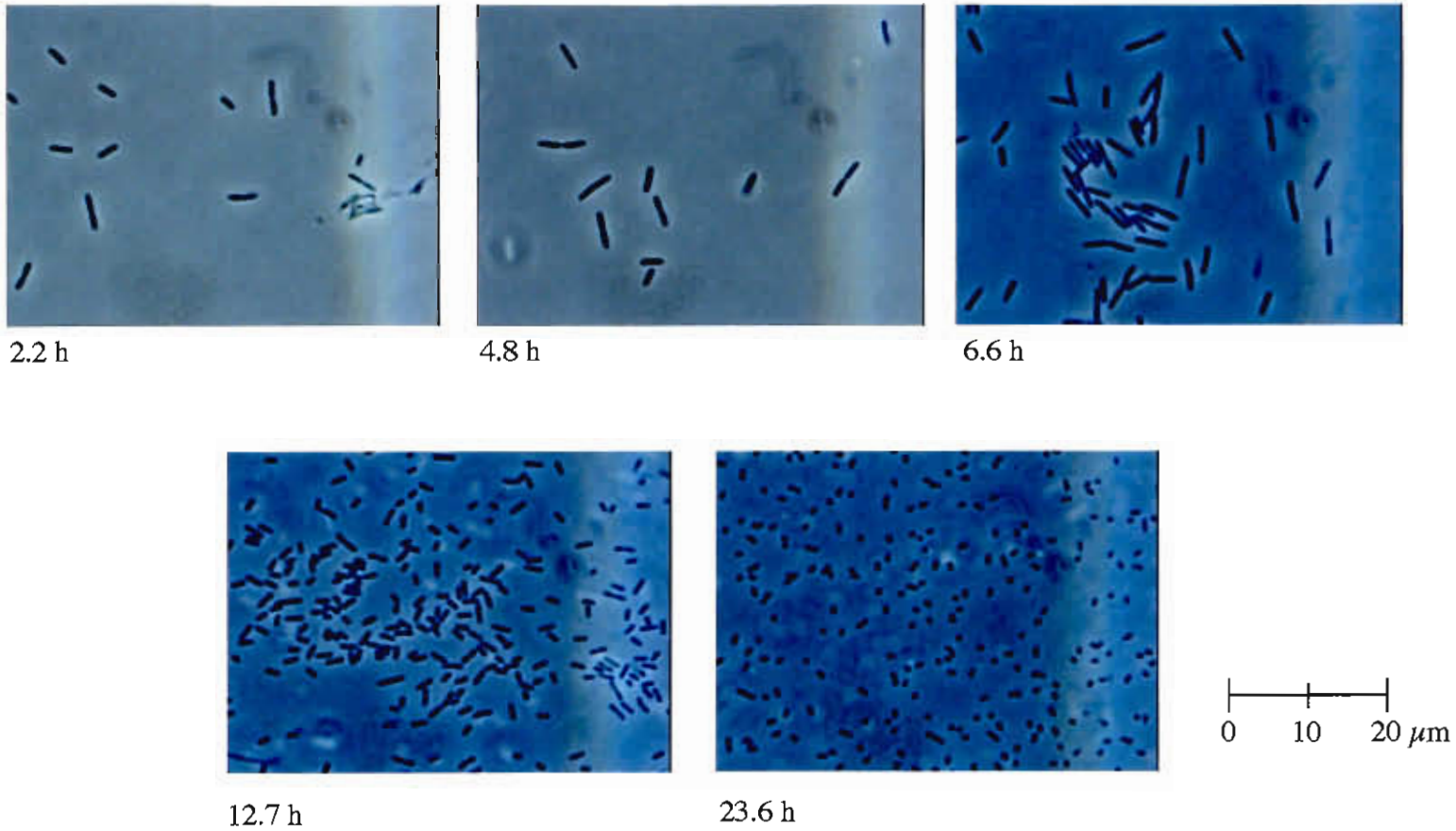

Figure 6a. *P. aeruginosa* at different stages of a batch culture (exponential phase: 2.2, 4.8, and 6.6 h; stationary phase: 12.7 and 23.6 h). The pictures were taken at time points indicated in Figure 5.

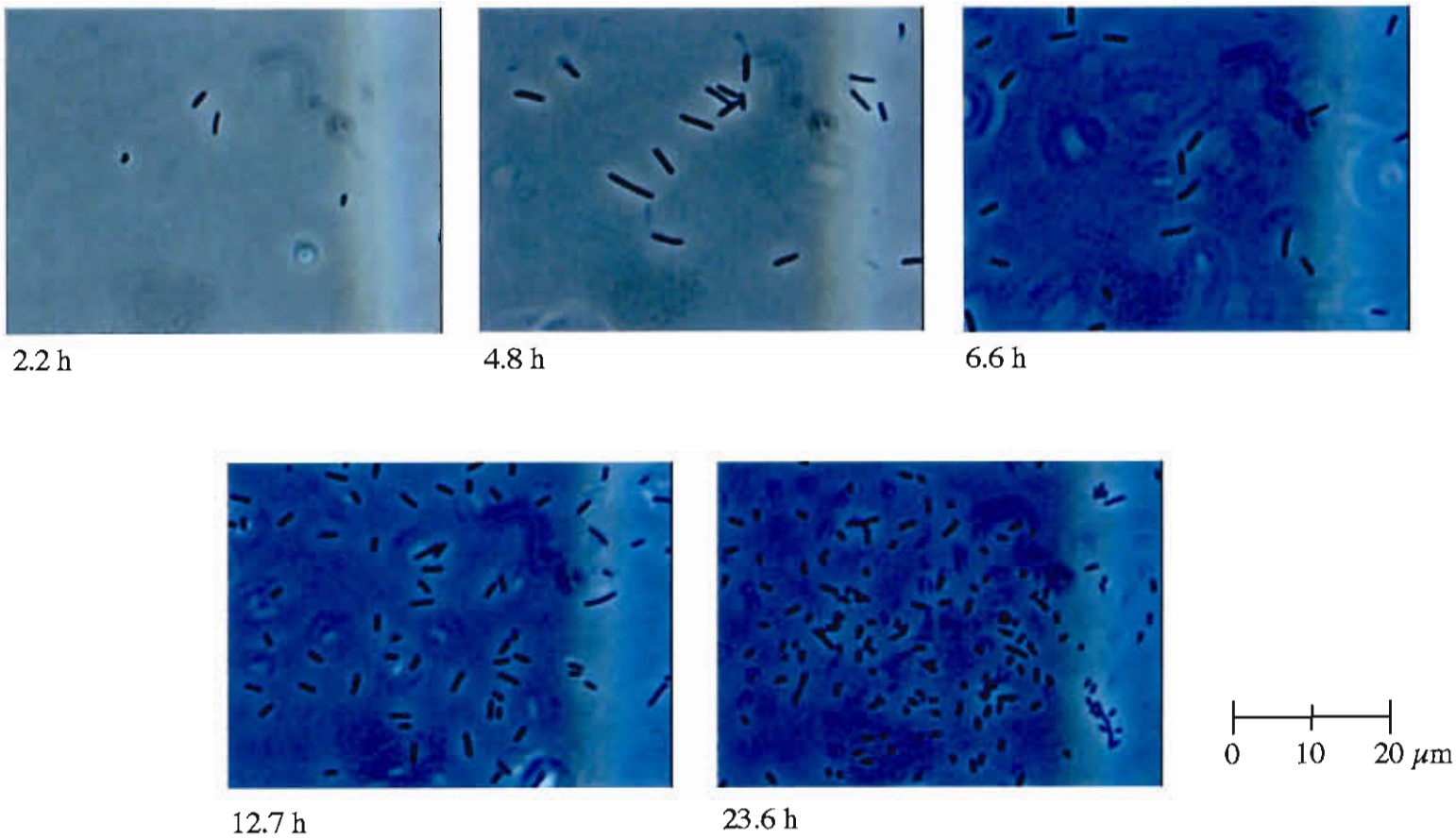

Figure 6b. *P. aeruginosa* at different stages of a batch culture containing 5 mM ZA (exponential phase: 2.2, 4.8, and 6.6 h; stationary phase: 12.7 and 23.6 h). The pictures were taken at time points indicated in Figure 5.

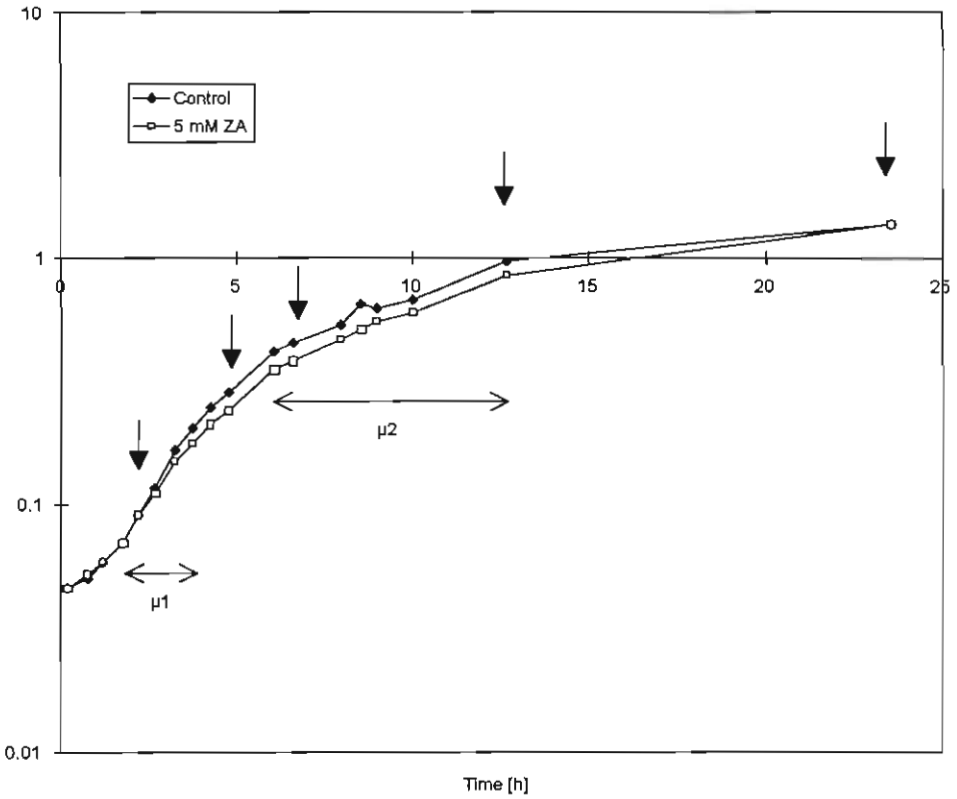

Figure 7. Batch of *S. aureus* in shake flask cultures with medium E2 and 1.8 g glucose l^{-1}. Two exponential growth phases (μ1 and μ2) could be observed for the ZA containing and the control culture (0 mM ZA). The arrows indicate the time points, when microscope pictures were taken (Fig. 8a and b).

There were two exponential growth phases detectable: μ1 and μ2 (Fig. 7). The specific growth rate differed significantly: the ZA containing culture grew at a rate of $\mu 1 = 0.46\ h^{-1}$, whereas the control without ZA grew faster at $\mu 1 = 0.55\ h^{-1}$. Both cultures grew in the second growth phase at $\mu 2 = 0.13\ h^{-1}$.

The pictures taken at time points indicated in Figure 7 are displayed in Figure 8a and b. It can be seen that the cells grown in presence of ZA (Fig. 8b) were less separated in the second exponential phase, however, they were again separated to single cells in the stationary phase (23.58 h). The control (Fig. 8a) showed a similar pattern. However, in the stationary phase the cells were loosely attached to each other. In general, there were fewer micro-colonies in the control than in the ZA culture.

Interpretation: ZA shows growth dependent influences:

ZA affects the growth only in the first exponential growth phase μ1, whereas the growth in the second phase did not differ. The cell morphology is changed in μ2: the ZA containing culture had large micro-colonies. However, in the stationary phase these colonies became smaller. Thus, the influence of ZA depends on the growth phase of *S. aureus*.

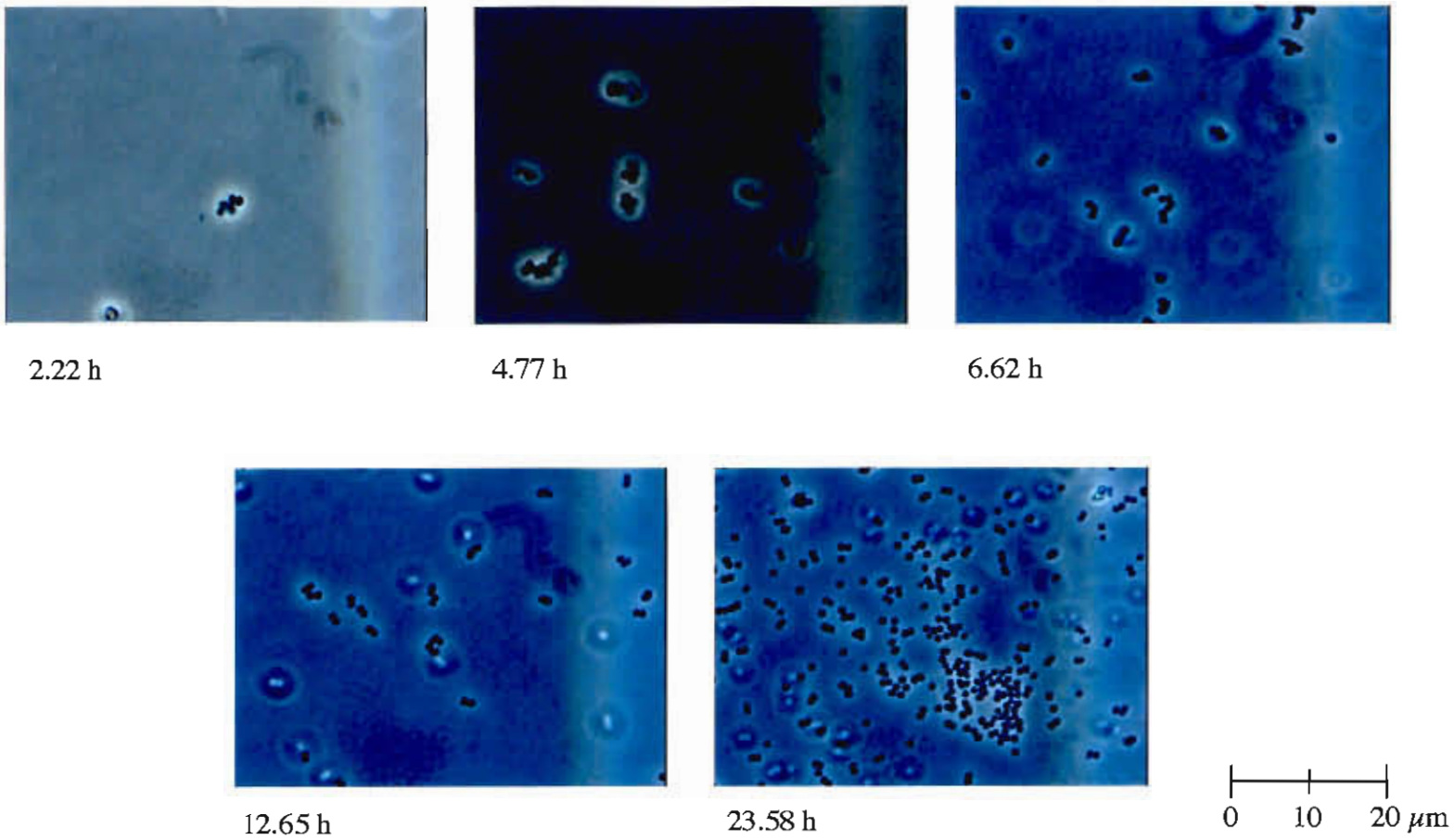

Figure 8a. *S. aureus* at different stages of a batch culture (exponential phase 1: 2.22, 4.77, exponential phase 2: 6.62 and 12.65 h; stationary phase: 23.6 h). The pictures were taken at time points indicated in Figure 7.

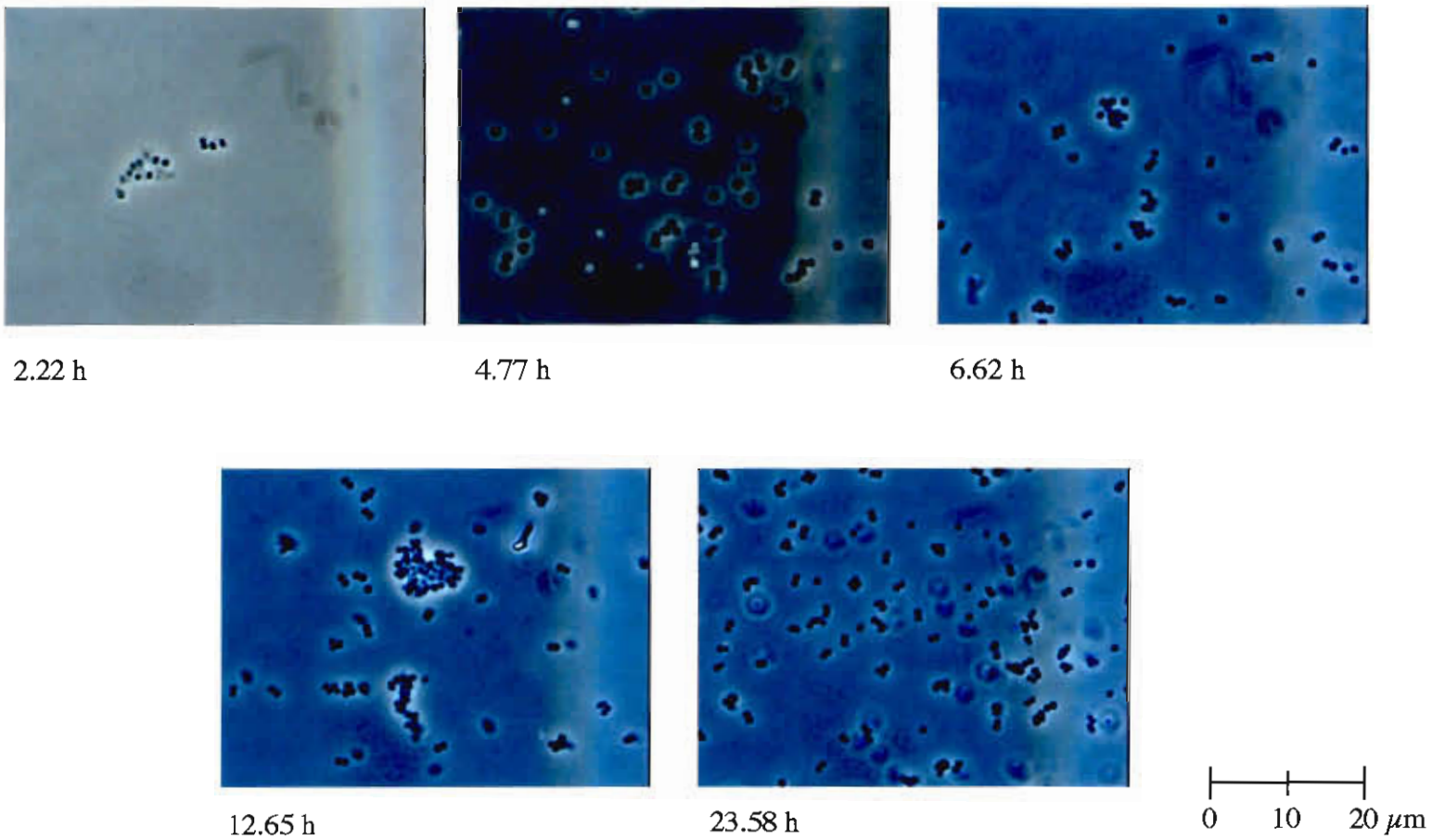

Figure 8b. *S. aureus* at different stages of a batch culture containing 5 mM ZA (exponential phase 1: 2.22, 4.77, exponential phase 2: 6.62 and 12.65 h; stationary phase: 23.6 h). The pictures were taken at time points indicated in Figure 7.

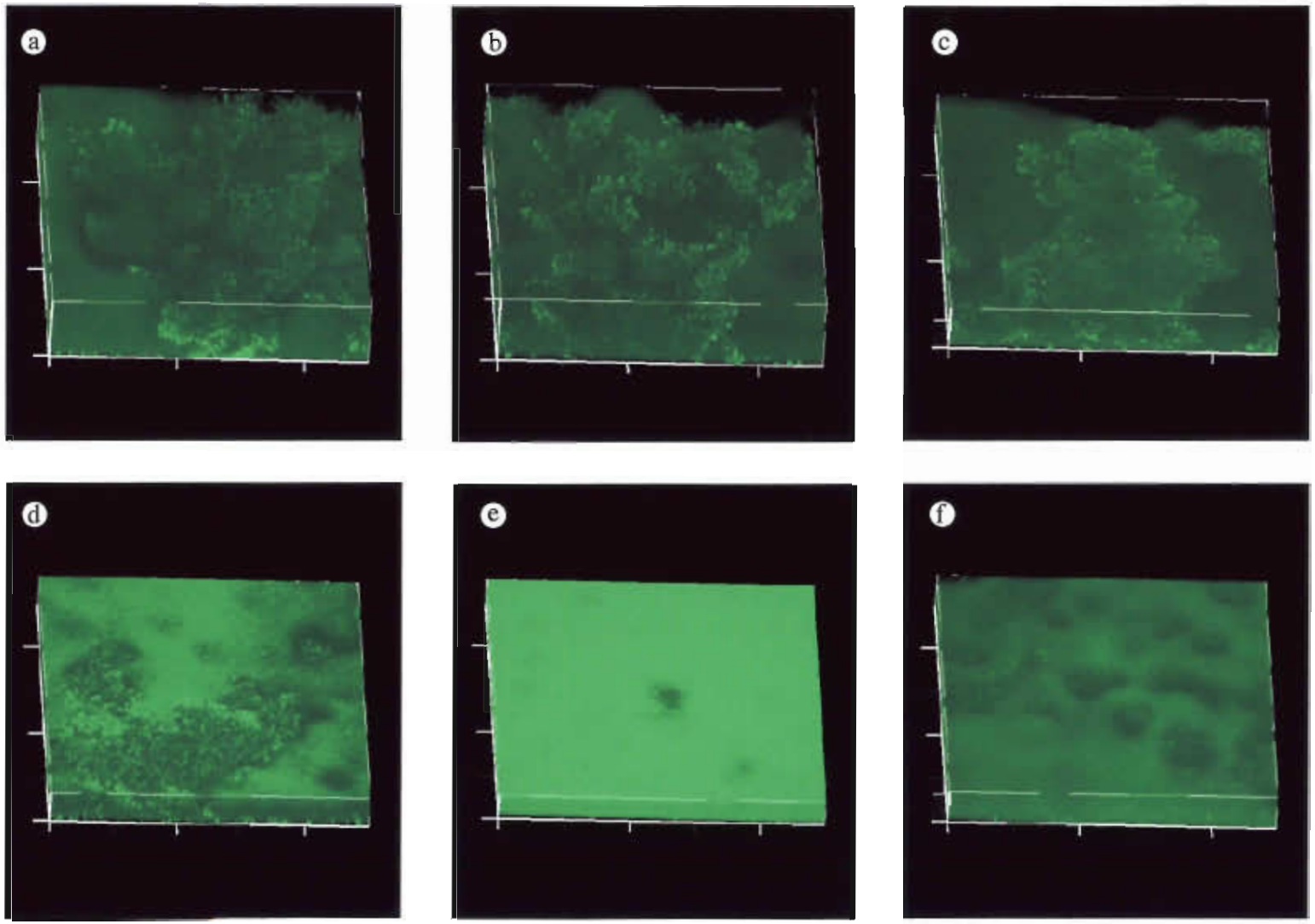

Figure 9. Biofilm of *V. harveyi* in a mini flowcell produced by continuous inoculation of a starved batch culture (a, b, and c) and in presence of 5 mM ZA (d, e, and f). The cells were stained with fluorescein and observed applying confocal microscopy. Dimensions: side lengths: 250 μm x 250 μm, thickness: a: 56 μm, b: 73 μm, c: 45 μm, d: 54 μm, e: 18 μm, f: 23 μm.

Cell attachment in mini-flowcells

V. harveyi

V. harveyi was grown in a chemostat with sea water complete medium at a dilution rate of 0.05 h^{-1}. Twice a volume of 50 ml culture broth was harvested and transferred into two Erlenmeyer flasks containing 100 ml sterile sea water with and without ZA (5 mM ZA end concentration). The cultures were stirred in order to avoid cell gradients in the flasks. Over a period of more than 14 hours, these starved cells were pumped through a mini-flowcell. Confocal microscopy showed that the biofilm thickness of the culture with ZA was considerably thinner (Fig. 9).

Interpretation: Cell attachment is reduced by ZA in this experiment.

S. aureus

S. aureus was grown in a shake flask on medium E2 with 1.8 g glucose l^{-1}. The culture was then split into two subcultures and diluted with medium E2 containing 5 mM ZA (end concentration was 2.5 mM ZA). While the cultures were growing, they were used as inocula for mini-flowcells. The flow rate was set to 0.275 ml min^{-1}. After 5 minutes of flow, the mini-flow cells were washed for 5 minutes with isotonic saline at the same pump rate. The flow-cells were subsequently examined under the microscope and the *S. aureus* cells were visually counted as described in material and methods. This cycle was repeated 3 times. After one cycle, the ZA culture showed a lower coverage number than the control. However, after 3 cycles the surface was more covered by ZA grown cells.

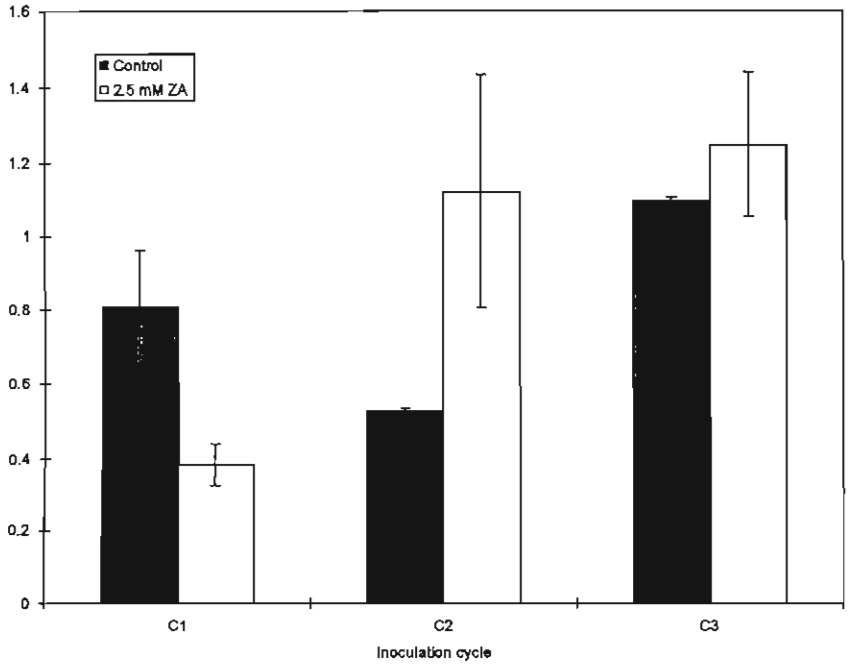

Figure 10. Coverage of *S. aureus* cells on the glass surface of a mini-flowcell after different inoculation cycles. The error bars represent 95 % confidence limits.

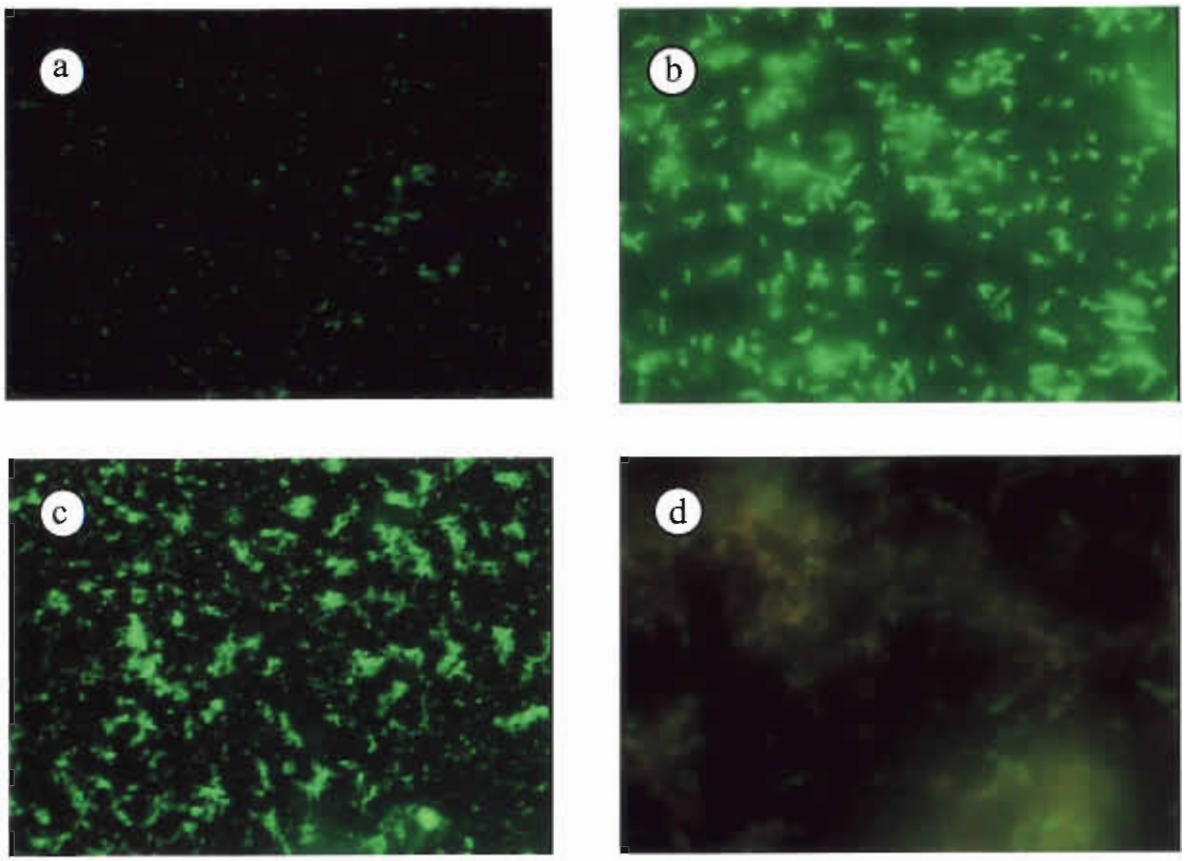

Figure 11. GFP containing *E. coli* attached to stainless steel coupons.
Panel a and b: control (no ZA); panel c and d: with 5 mM ZA.
Magnifications: 10x (through air-water interface): a and c; 60x (water-immersion objective): b and d.

Interpretation: The interpretation of the result is rather difficult, because the *S. aureus* cells went through different growth phases during the inoculation of the mini-flowcells. It can be speculated that the cells of the first cycle represent growing cells of the late exponential phase 1 (Fig. 7), whereas the cycles 2 and 3 are in the phase 2 (μ2). Thus, a reduced attachment of *S. aureus* can be expected for growth in presence of ZA.

Cell attachment in large flowcells

Attachment of E coli *on stainless steel coupons*

Two chemostats were ran with the same medium (medium E2 with 0.11 g l^{-1} glucose), however, one culture was growing in presence of 5 mM ZA. The dilution rate was 0.25 h^{-1} in both cases. Each chemostat was connected to a large flowcell that contained 5 stainless steel coupons. The flowcells were continuously inoculated for 15 minutes (feed concentration: $1.5*10^9$ cells ml^{-1} for the control and $3.6*10^9$ cells ml^{-1} for the ZA containing culture; feed rate 5.4 ml min^{-1}; dilution rate: 4.3 h^{-1}). Before each fluorescence reading the flowcells were flushed with buffered glucose (0.18 g glucose l^{-1}, pH 7.0) at the same pump rate for 30 minutes. This cycle was repeated three times and the flowcells were taken apart. The first coupon of each flowcell was investigated under the microscope.

The GFP-signals (Fig. 12) showed a steady increase of the fluorescence. The sequence of the signal showed a steeper slope of increase for the ZA containing culture. This observation can be explained by the denser inoculum.

Pictures of the first (downstream) coupon of the flowcells showed a clear difference in the structure of the attached cells. The ZA containing culture had more clumped cells than the control culture (Fig. 11).

The viable cell counts were in accordance to the fluorescence signals (data not shown).

Interpretation: ZA makes the cells clump on stainless steel coupons.

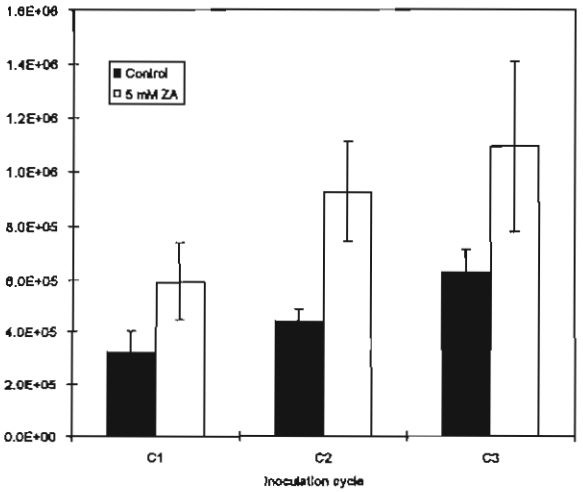

Figure 12. Total fluorescence signal of green fluorescent protein in a flowcell experiment with *E. coli* M182. The signal was averaged over the whole flowcell and the error bars represent the standard deviation of the data.

Antifoulant efficiency

Detachment experiments of cells on ZA/silicone coated metal coupons

The application of large flowcells enabled the study of cell growth on surfaces. The test surfaces were silicone coatings with different ZA contents (0, 5, 10, and 25% ZA). After inoculation over 4 hours the growth of the biofilm was followed by the measurement of the tryptophan fluorescence (biomass indicator) and natural bioluminescence (cell activity).

The bioluminescence increased during the whole experiment, whereas the tryptophan signal was influenced by ZA and could not be used as biomass indicator.

After 96 hours the shear stress was increased from 3 to 330 dynes cm^{-2} and cells on the coupons were harvested using probe sonication. The cell number (AODC) between the ZA treated and untreated silicone coupons did not differ significantly, however, lipid analysis (Microbial Insights, TN) revealed that the cells on the ZA coupons grew slower (cy19:0/18:1w7c) and were less stressed (18:1w7t/18:1w7c) in comparison to the reference metal coupons.

Interpretation: ZA does not harm the cells, however, the growth rate is reduced.

Biofouling of 4-PPAS/silicone coated metal coupons

V. harveyi was grown in a chemostat in supplemented ASW medium. The experiment was set up in the same way like repeated with polymerized ZA (4-PPAS, 4-pentyl-phenyl acid sulfate) in silicone coupons (0 and 20% w/w).

The bioluminescence of the coupons increased. After 96 hours, (no shear stress was performed) the cell number on the treated silicone coupons was lowered by 57 ± 24% in comparison to untreated ones.

Lipid data showed a reduction of biomass (Tab. 3) on 4-PPAS treated coupons. Unfortunately, the biomass was too low to investigate the lipid pattern.

Interpretation: 4-PPAS is an efficient antifoulant, however, more experiments are needed to achieve better lipid data.

Table 3. Total extracted lipid of coupons in an antifoulant experiment with *V. harveyi*.

Sample	Extracted lipids (control) [pmol][a]	Extracted lipids (4-PPAS) [pmol][b]
Coupon 3	377 ± 295	100 ± 14
Coupon 4	328 ± 305	6 ± 6
Coupon 5	110 ± 126	272 ± 169

[a] The coupon at the position 4 was coated by silicone RTV11. Coupons 3 and 5 were polished stainless steel.
[b] The coupon at the position 4 was coated by a mixture of silicone RTV11 with 4-PPAS (20% w/w). Coupons 3 and 5 were polished stainless steel.

4. References

Arrage, A. A., Vasishtha, N., Sundberg, D., Bausch, G., Vincent, H. L. and White, D. C. 1995. On-line monitoring of antifouling and fouling-release surfaces using bioluminescence and fluorescence measurements during laminar flow. J. Indus. Microbiol. **15**: 277-282.

Arrage, A. A. and White, D. C. 1997. Monitoring biofilm-induced persistence of *Mycobacterium* in drinking water systems using GFP fluorescence, pp. 383-386. In: J. W. Hastins, L. J. Kricka and P. E. Stanley (eds.), Bioluminescence and Chemiluminescence: Molecular Reporting with Photons, John Wiley & sons, New York.

Hastings, J. W. and Nealson, K. H. 1981. Bacterial bioluminescence. Ann. Rev. Microbiol. **31**: 549-595.

Lageveen, R. G., Huisman, G. W., Preusting, H., Ketelaar, P., Eggink, G. and Witholt, B. 1988. Formation of polyesters by *Pseudomonas oleovorans*: effect of substrates on formation and composition of poly-(*R*)-3-hydroxyalkanoates and poly-(*R*)-3-hydroxyalkenoates. Appl. Environ. Microbiol. **54**: 2924-2932.

Mittelman, M. W., Packard, J., Arrage, A. A., Bean, S. L., Angell, P. and White, D. C. 1993. Test systems for determining antifouling coating efficacy using on-line detection of bioluminescence and fluorescence in a laminar-flow environment. J. Microbiol. Methods **18**: 51-60.

Palmer, R. J. and Caldwell, D. E. 1995. A flowcell for the study of plaque removal and regrowth. J. Microbiol. Methods **24**: 171-182.

Palmer, R. J., Phiefer, C., Burlage, R., Sayler, G. and White, D. C. 1997. Monitoring biofilm-induced persistence of *Mycobacterium* in drinking water systems using GFP fluorescence, pp. 445-450. In: J. W. Hastins, L. J. Kricka and P. E. Stanley (eds.), Bioluminescence and Chemiluminescence: Molecular Reporting with Photons, John Wiley & sons, New York.

C. Interaction of Zosteric Acid with Synthetic Polymer Coatings

Gill Geesey
Center for Biofilm Engineering, Montana State University Bozeman, MT 59717-3980

1. Goal:

The goal of this portion of the research was to prepare synthetic polymer coatings on substrata for evaluation of the antifouling properties of zosteric acid (ZA)

2. Summary of Results and Accomplishments

Stainless steel coupons were dip-coated in polystyrene (PS) or poly-octadecylmethacrylate (POMA) and sent to Professor D.C. White for use in bacterial colonization studies. The outcome of those studies are reported elsewhere in this report.

The infrared (ir) spectrum of ZA was determined as a preliminary step for the study of its adsorption to surfaces from aqueous media. Figure 1 shows the ir spectrum of a 3 mg/ml aqueous solution of ZA collected by attenuated total reflectance Fourier transform infrared spectroscopy (ATR/FT-IR) after subtraction of the water. Characteristic sulfate and carboxylate functionalities were clearly detectable.

Thin films of PS and POMA were spin cast on germanium internal reflection elements (Ge IRE). A drop of a 1% solution of each polymer in toluene was place on a trapezoidal Ge IRE that was mounted in a chuck on the spindle of a centrifuge and rotated at 1000 rpms for 5 min to achieve a smooth, continuous film. Film stability in the presence of a stream of water was determined by following the intensity of the ir water absorption band at 1650 cm^{-1}over time. The films appeared to remain intact and stable under these conditions.

Adsorption of ZA from aqueous phase to POMA and PS films on a Ge IRE was determined. ZA (3 mg/ml) in both tap water and deionized water adsorbed reversibly to POMA. (Figure 2 and 3). Adsorption of ZA from aqueous phase to PS films was compared with that of other solutes. Initial studies indicated that ZA as a 3 mg/ml aqueous solution adsorbed to PS films in a reversible manner similar to glucose (Figure 4). For comparison, a slowly desorbing compound, ciprofloxacin, is included (Figure 4). The reversible adsorption of ZA to PS was not repeatable after these initial experiments, however. Subsequent adsorption studies repeatedly showed ZA adsorbing from deionized water and phosphate buffer solutions at pH 7.0 on PS films, leaving a reside that yielded an ir spectrum similar but not identical to solution phase ZA after extensive rinsing with ZA-free aqueous phase (data not shown). The irreversibly adsorbed ZA caused the PS film to become noticeably more hydrophilic and more strongly bonded to a Ge substratum.

Thin films of ZA-containing PS were spin cast on germanium internal reflection element (IRE) and the stability of the films and leaching of ZA evaluated by ATR/FT-IR. as described above for the pure polymer films. ZA-incorporated PS films were prepared by

adding 200 µl of a 10 mg/ml solution of ZA in methanol to 3.6 ml of a 1% solution of PS on tetrahydrofuran and the resulting mixture spin-coated on the Ge IRE as described above. By comparing the spectrum of the ZA-incorporated PS film (Figure 5a) with that obtained from a film of pure PS (Figure 5b) and that obtained for ZA by itself (Figure 5c), it can be shown that ZA was incorporated into the PS film. Upon exposure of the film to a flowing stream of water, it was determined that 90% of the ZA was leached out over a 90 min period.

Glass surfaces were also spin-coated with a thin film of PS with and without ZA incorporated into the polymer film as described above for Ge IREs. The polymer-coated glass substrata were used to assess the influence of ZA on substratum colonization and fouling by bacteria as described below.

The influence of ZA on the behavior of suspended bacterial populations was determined prior to an evaluation of its influence on bacterial adhesion to surfaces. When introduced as the sole carbon source to a defined marine culture medium, ZA did not promote the growth of the marine chemoorganotrophic bacteria *Pseudoalteromonas atlantica* and an *Oceanospirillum sp.* Based on this limited data set, it appears that ZA is not a common carbon or energy source for marine bacteria and thus may be relatively resistant to biodegradation in the marine environment.

In a defined medium, known to support the growth of these bacteria, ZA had a significant influence on the growth rate of P. atlantica. In the absence of ZA batch cultures of. exhibited a maximum specific growth rate (□□□of $0.36 h^{-1}$, whereas, in the presence of 300 □g l^{-1}, the maximum specific growth rate in the same medium increased to $0.65 h^{-1}$ even though it had previously been shown not to serve as a carbon or energy source for the bacteria (Figure 6). Oceanospirillum sp. did not exhibit a significant growth rate response to ZA, with κ values of 0.26 and $0.30 h^{-1}$ in the presence and absence of 300 µg l^{-1} ZA, respectively (Figure 7).

The effect of ZA on the growth of the freshwater bacterium *Pseudomonas aeruginosa* in glucose medium was also determined. In the presence of 1 mg/ml ZA, there was no apparent effect on the maximum growth rate of the organism (Figure 8).

A series of studies was performed to evaluate the influence of ZA on adhesion of P. aeruginosa to PS. A bacterial cell suspension was exposed to ZA either in solution or incorporated into the PS film. Cells exposed to ZA in solution for periods ranging from 1-96 h at 4C (to prevent growth) were subsequently exposed to a ZA-free, PS-coated surface at 25C for periods ranging from 0.5 to 1.5 h and the densities of attached cells determined by direct enumeration using epifluorescence microscopy after staining with DAPI. Bacterial cells exposed to surfaces with PS films incorporating ZA were not exposed to ZA in solution at 4C prior to exposure to the films for periods ranging from 0.5-1.5 h at 25C. The densities of cells attached to the surfaces under the conditions described above were compared to those obtained on ZA-free PS films when ZA was also absent from the bulk aqueous phase.

Pre-exposure to ZA at 4C led to enhanced cell attachment during 1.5 h exposure periods to ZA-free PS films than if the cells were never exposed to ZA (Table 1). Duration

of pre-exposure to ZA did not have much influence on the enhanced adhesion phenomenon. Pre-exposure to ZA for periods of 1-3 h resulted in a 2- to 3-fold increase in adhesion, while 4-96 h pre-exposure to ZA led to a 5-fold increase in adhesion.

Incorporation of ZA into the PS film produced variable results in terms of influence on cell adhesion. Of the 8 experiments conducted, 2 yielded densities of attached cells on Za-free and ZA-containing PS films that were comparable, 1 yielded cell densities on ZA-containing films that were 2 times higher than those on ZA-free films, and 5 yielded cell densities on ZA-containing films that were 2-3 times lower than those on ZA-free PS films (Table 1). The differences were smaller as the exposure time was reduced. The inconsistency of these results may be due to inconsistencies in ZA incorporation and leaching from the PS film. Surface chemical analyses should be conducted to resolve this question.

In summary, ZA displays some tendency to inhibit bacterial attachment to surfaces when it is incorporated into the substratum but promotes attachment of bacteria when dispersed in the bulk aqueous phase at concentrations of 300 μg/ml. These results offer a direction to pursue in the development of strategies for use of naturally-occurring, non-toxic substances to discourage biofouling of synthetic polymer surfaces.

Fig.1 FT-IR spectrum of zosteric acid

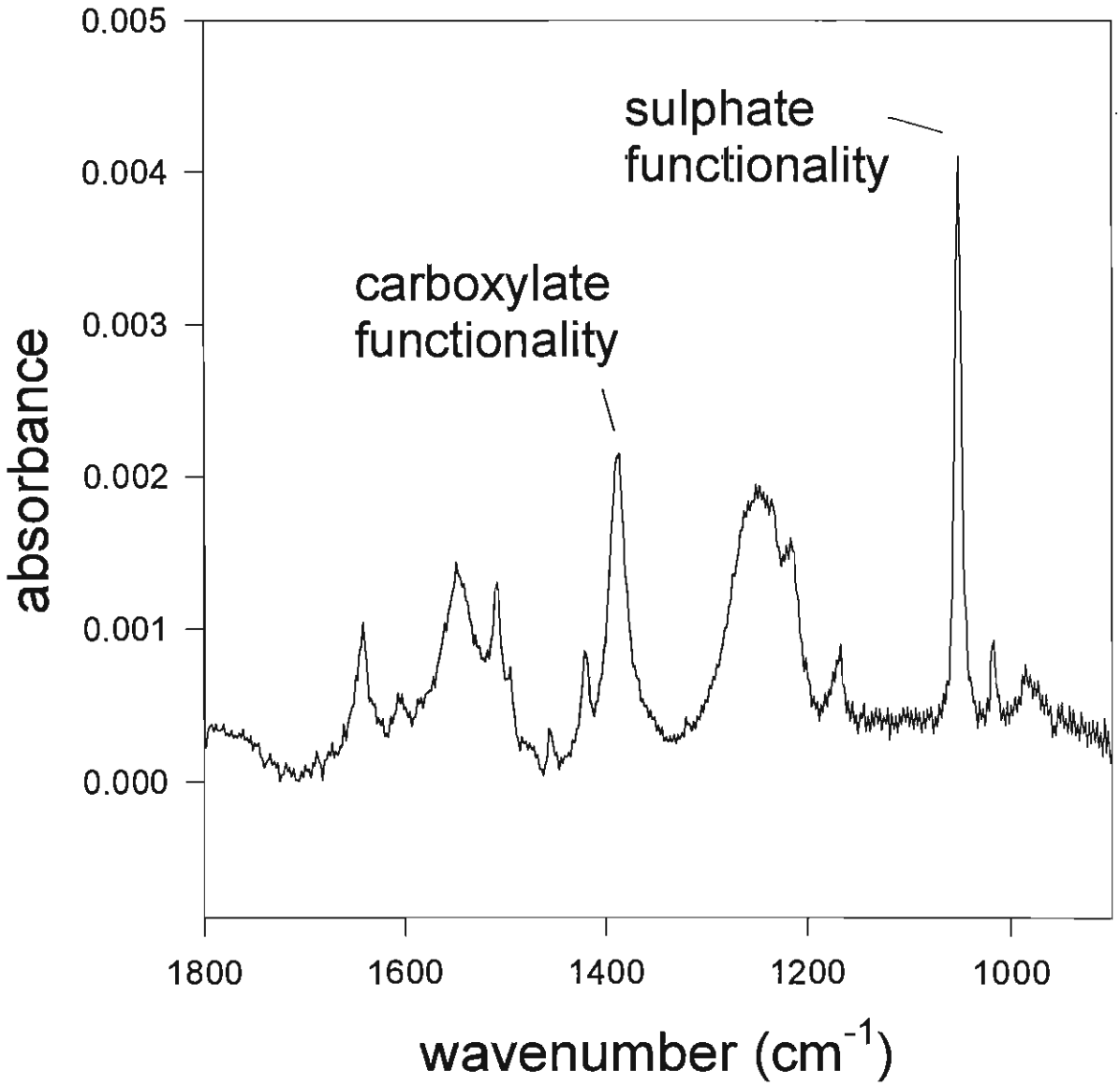

Fig 2. ZA (3mg/ml) on POMA in tap water

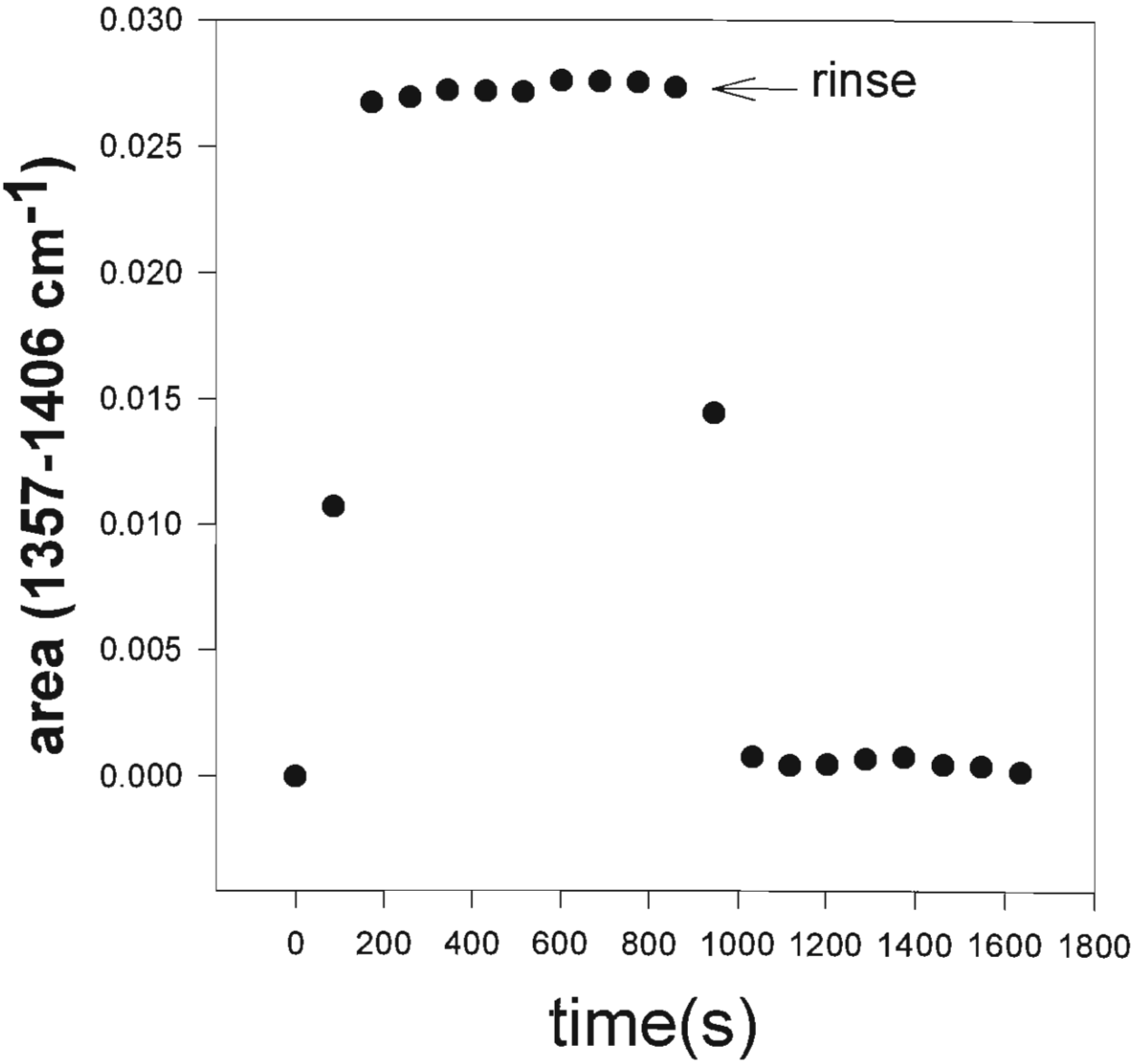

Fig.3. ZA (3mg/ml) on POMA /DI water

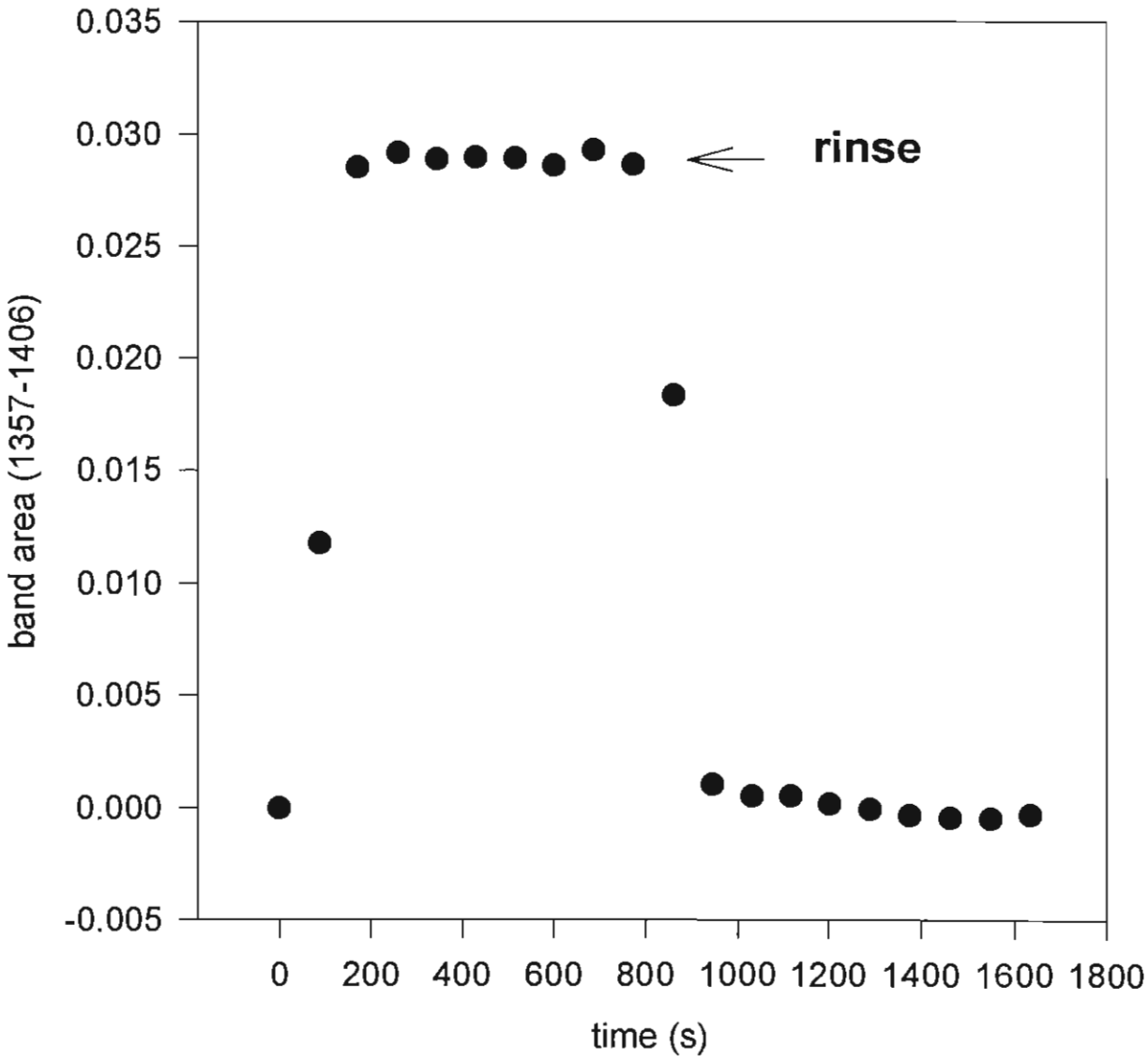

Fig.4 Kinetics of appearance & disappearance at polystyrene/aqueous interface

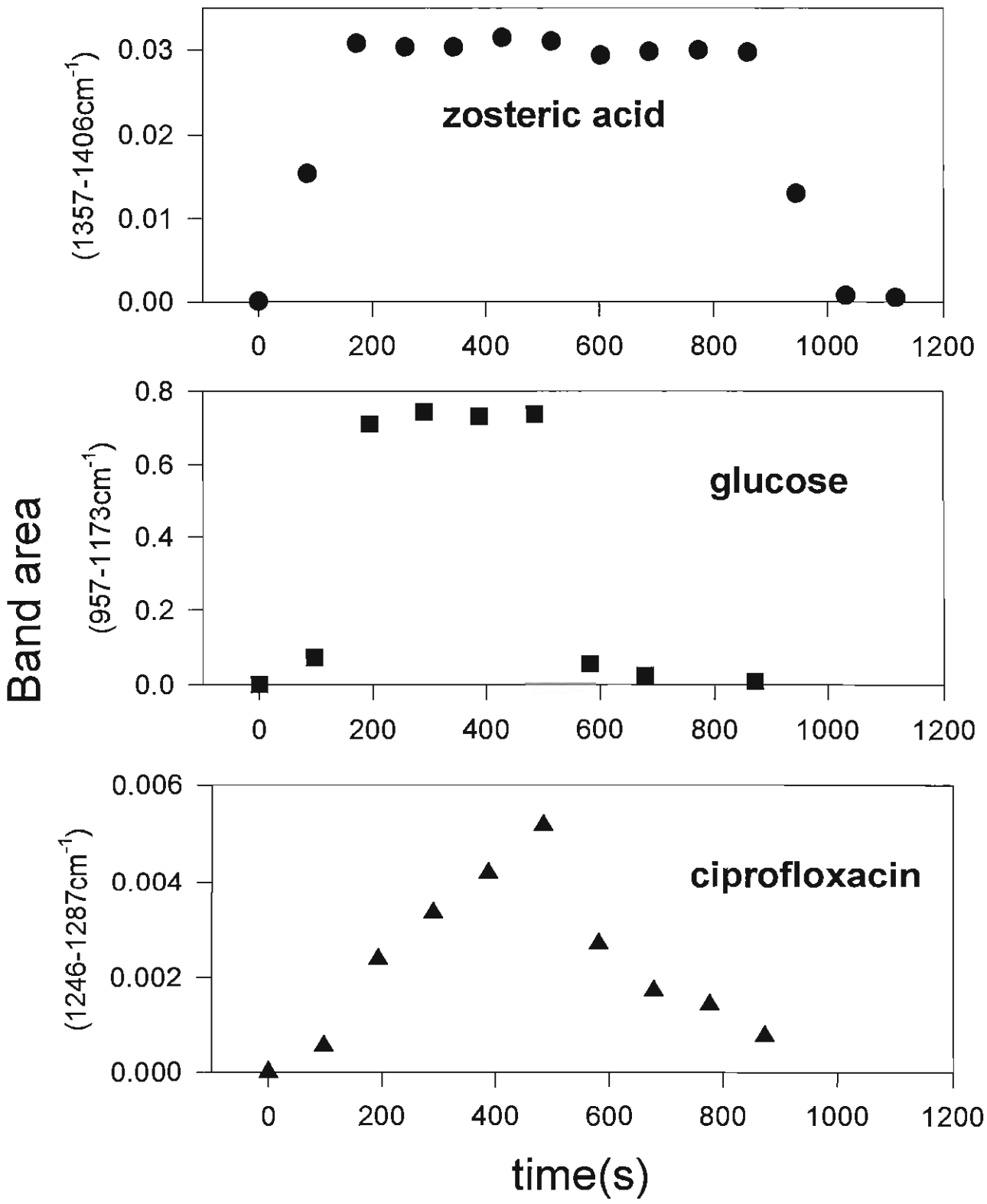

Fig.1 FT-IR spectrum of zosteric acid

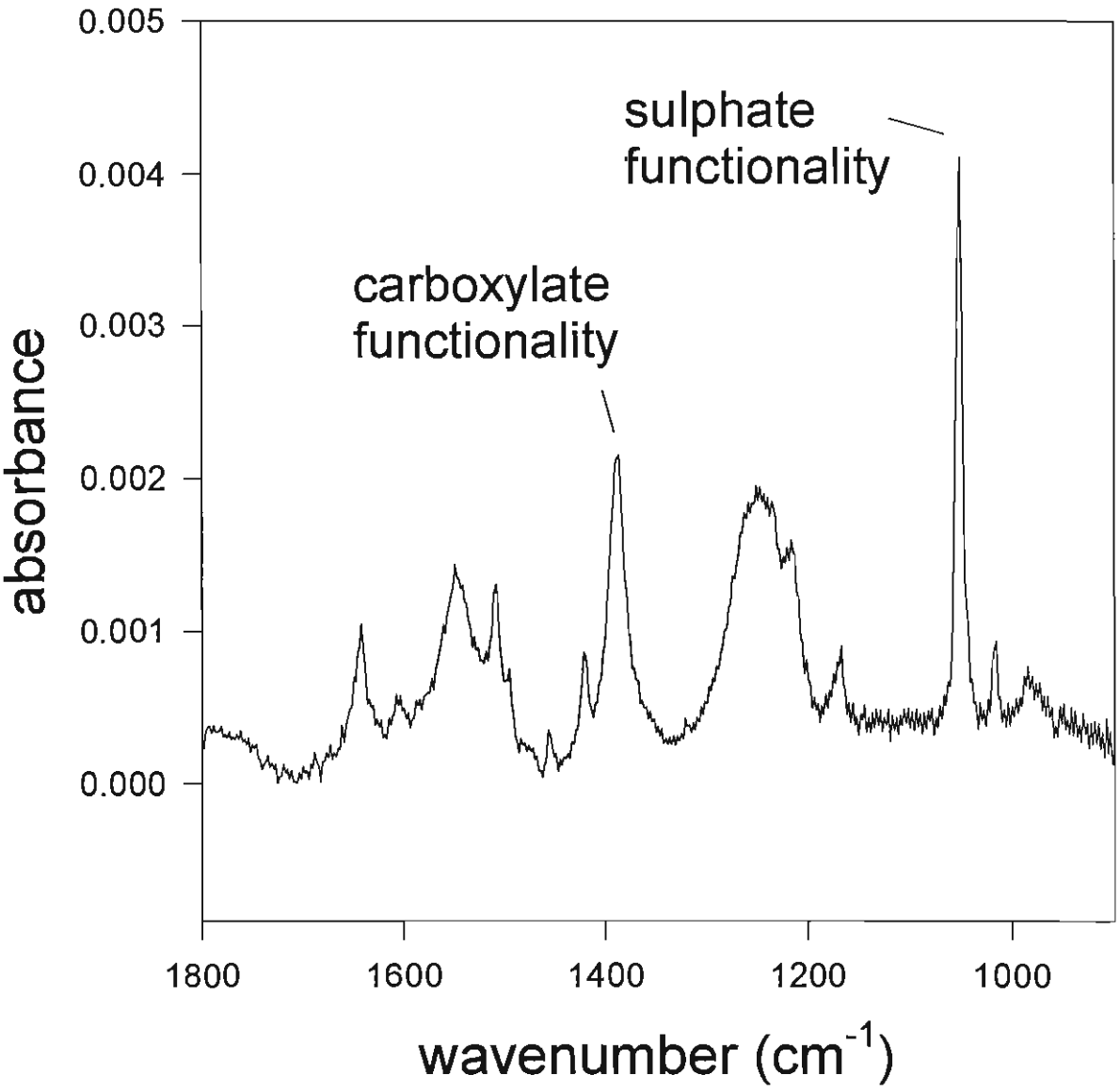

Fig 2. ZA (3mg/ml) on POMA in tap water

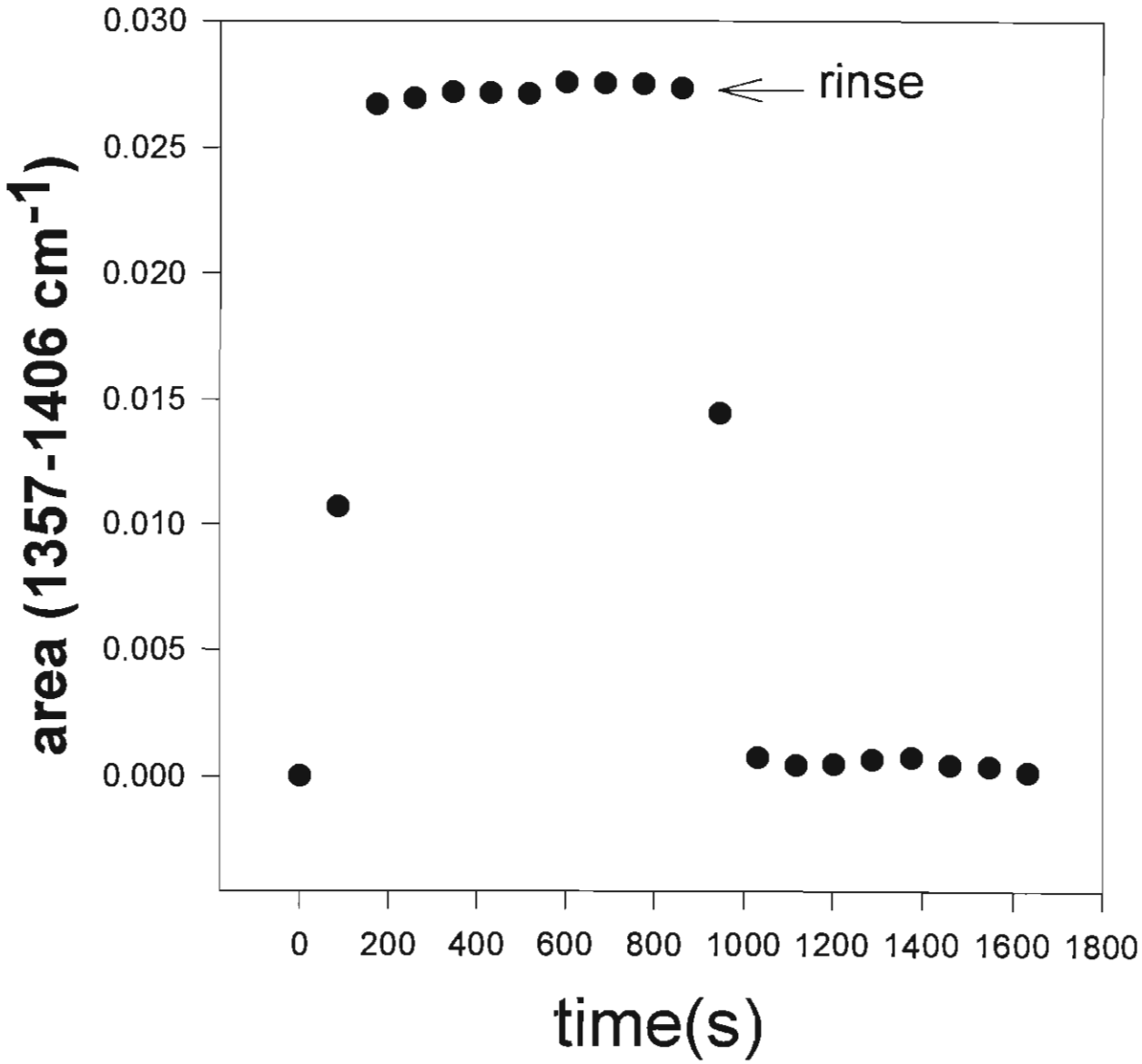

Fig.3. ZA (3mg/ml) on POMA /DI water

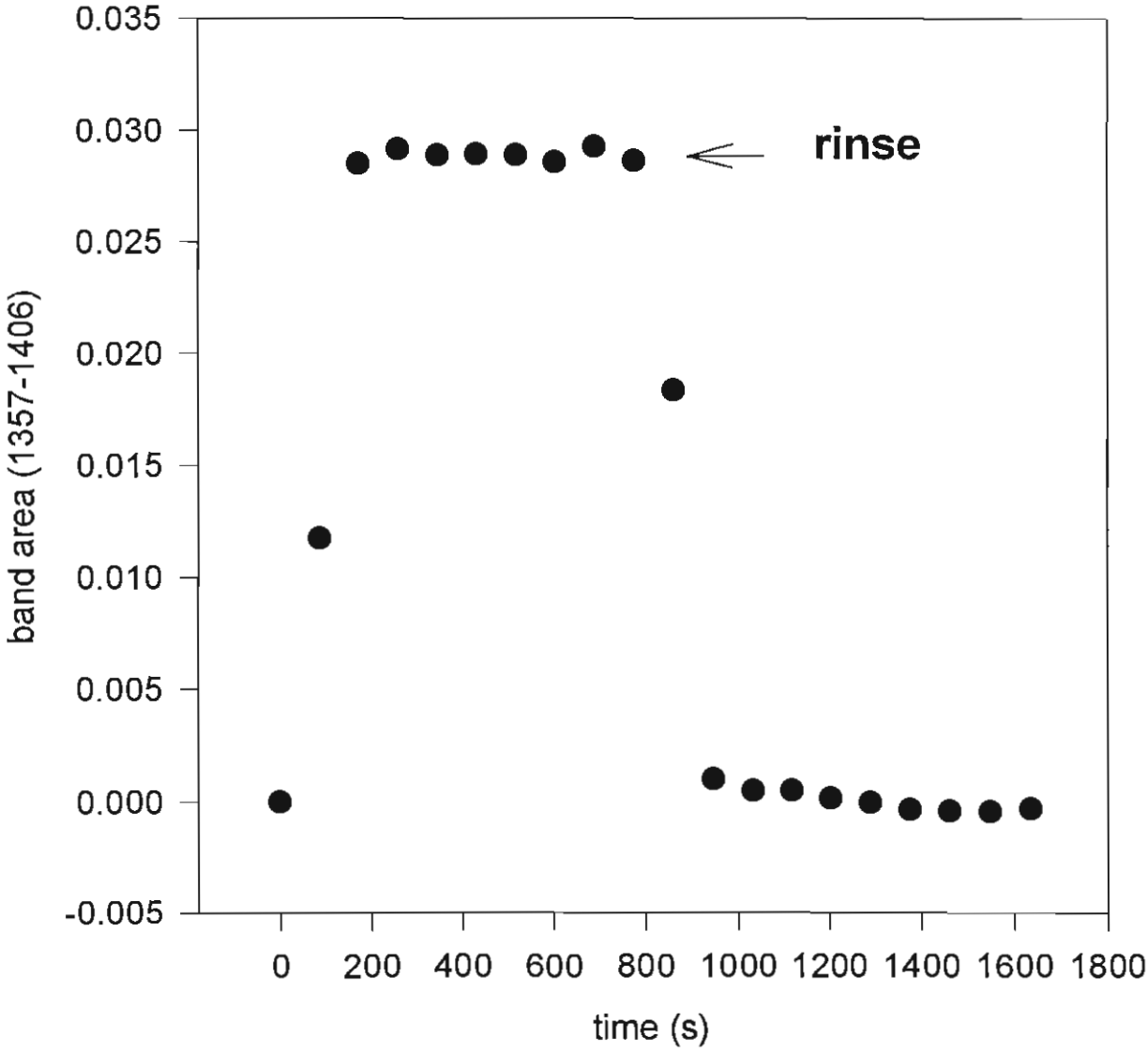

Fig.4 Kinetics of appearance & disappearance at polystyrene/aqueous interface

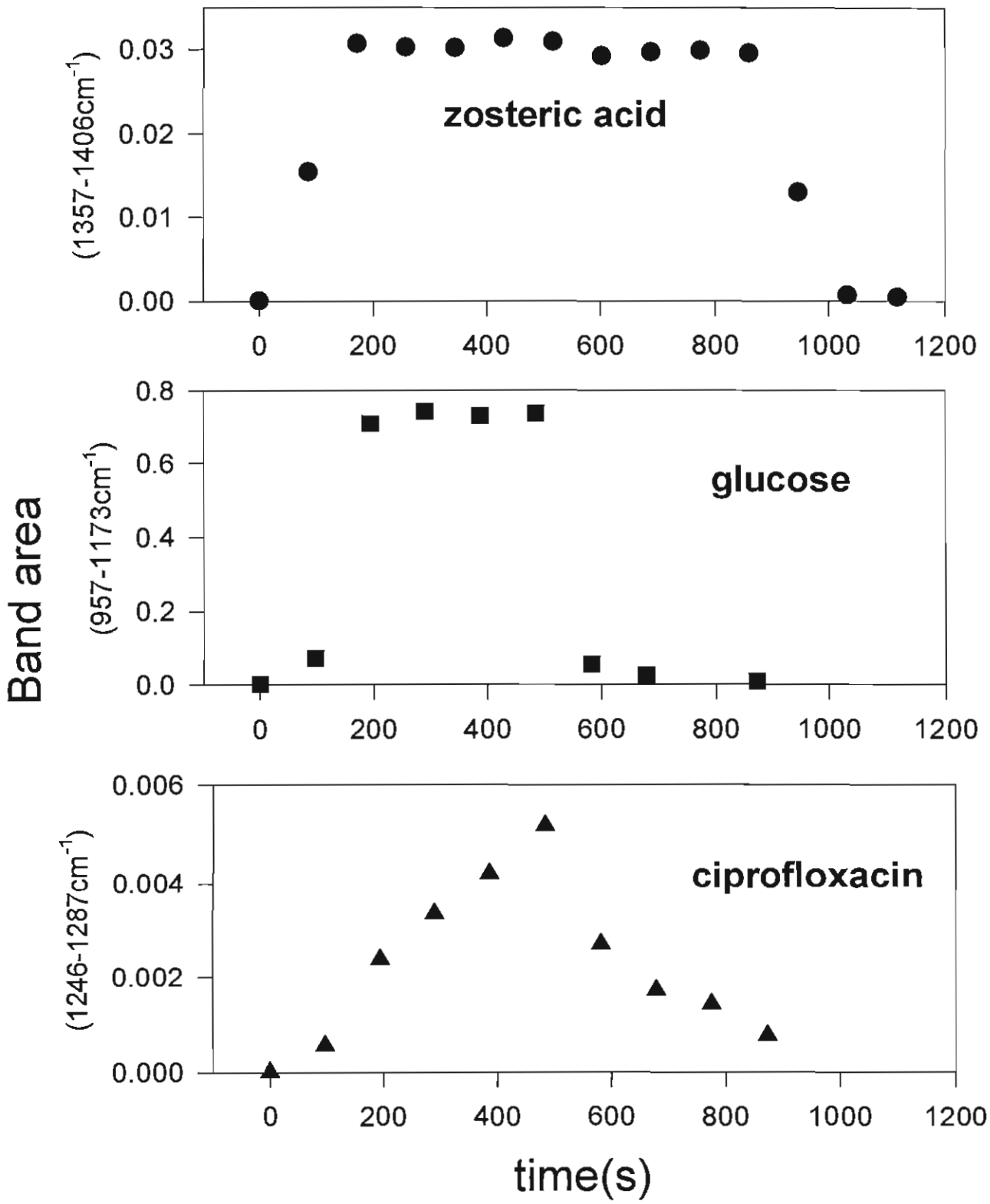

Fig.5

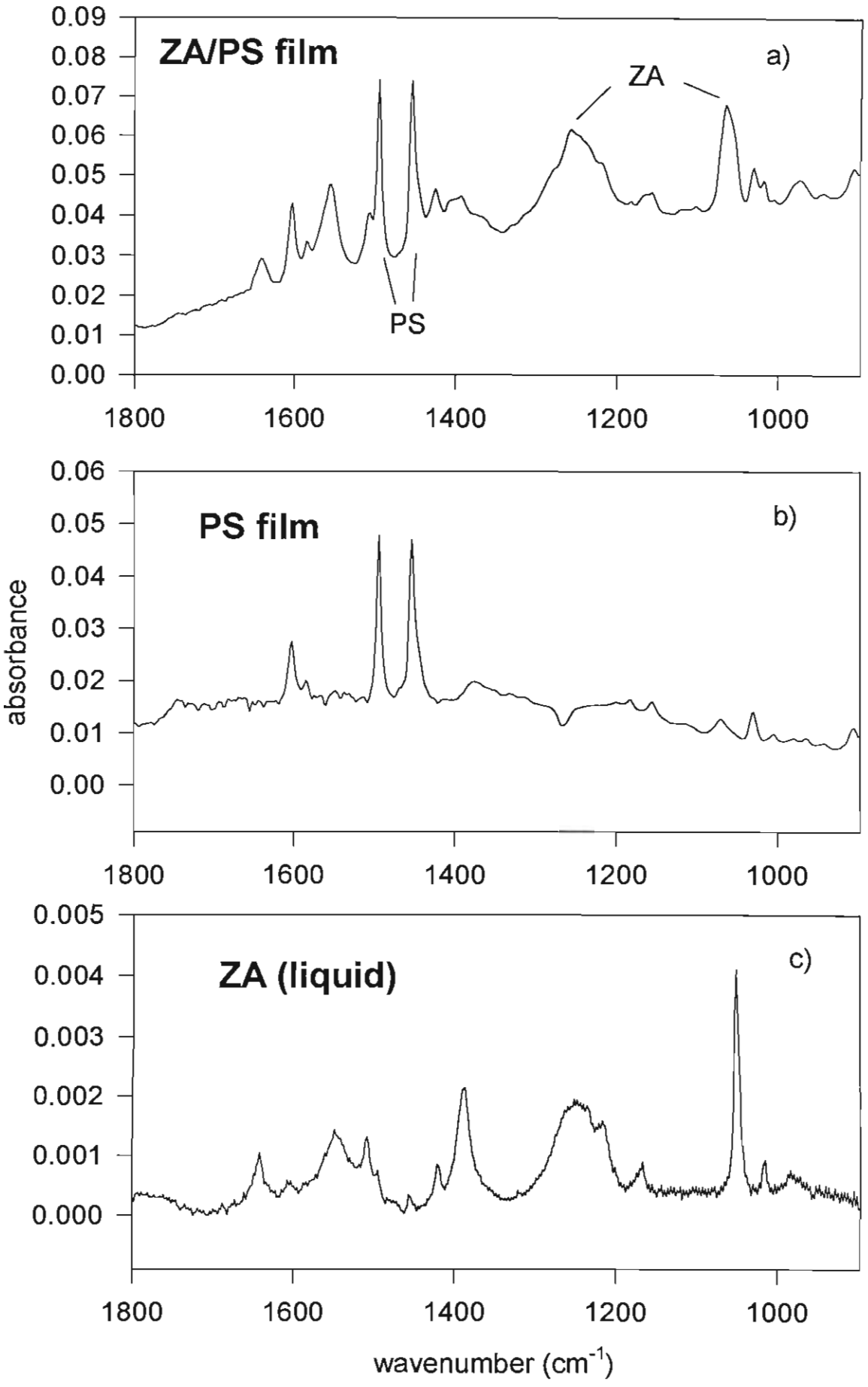
ZA/PS film
a)
ZA
PS
PS film
b)
ZA (liquid)
c)
absorbance
wavenumber (cm-1)
0.09
0.08
0.07
0.06
0.05
0.04
0.03
0.02
0.01
0.00
0.005
0.004
0.003
0.002
0.001
0.000
1800
1600
1400
1200
1000

Figure 6

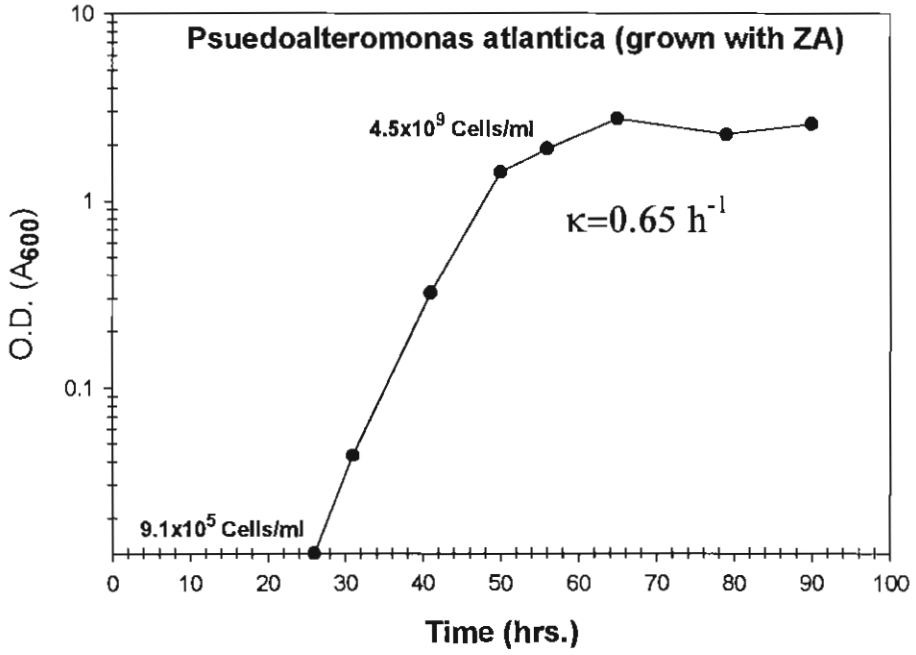
Psuedoalteromonas atlantica (grown with ZA)
4.5x10^9 Cells/ml
κ=0.65 h^-1
9.1x10^5 Cells/ml
O.D. (A600)
Time (hrs.)
10
1
0.1
0
10
20
30
40
50
60
70
80
90
100

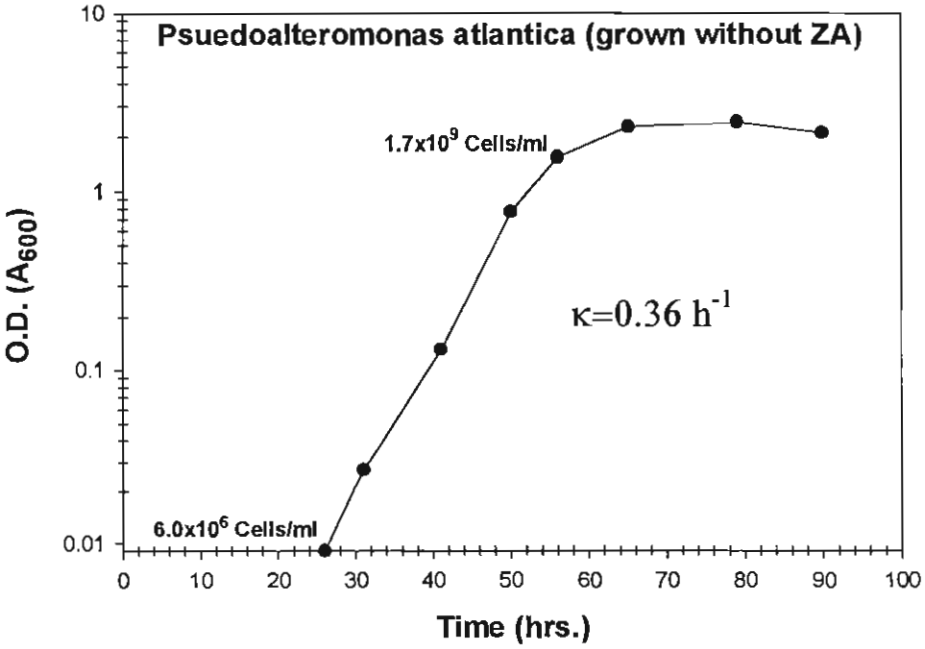
Psuedoalteromonas atlantica (grown without ZA)
1.7x10^9 Cells/ml
κ=0.36 h^-1
6.0x10^6 Cells/ml
O.D. (A600)
Time (hrs.)
10
1
0.1
0.01
0
10
20
30
40
50
60
70
80
90
100

Figure 7

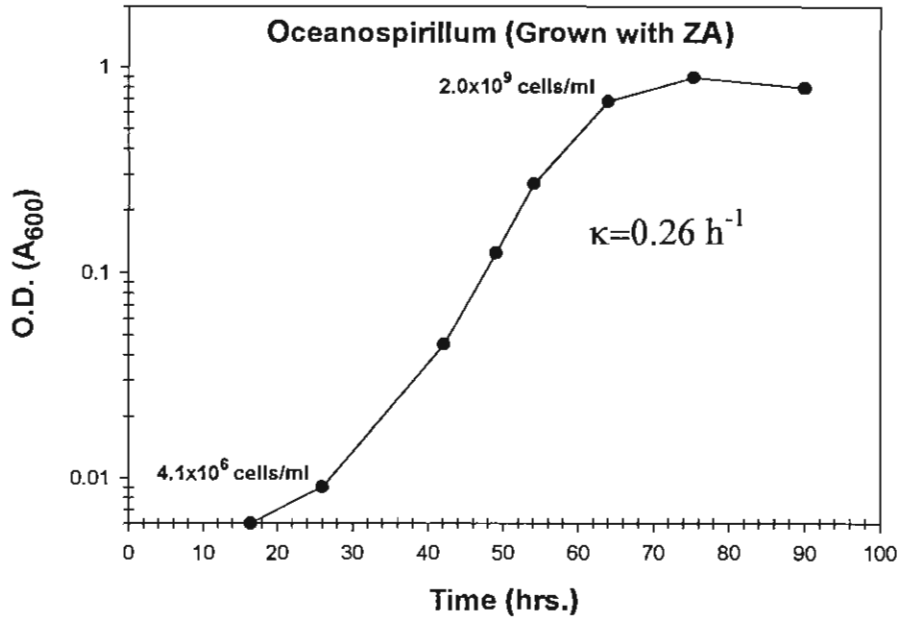
Oceanospirillum (Grown with ZA)
2.0x10^9 cells/ml
κ=0.26 h^-1
4.1x10^6 cells/ml
O.D. (A600)
1
0.1
0.01
0
10
20
30
40
50
60
70
80
90
100
Time (hrs.)

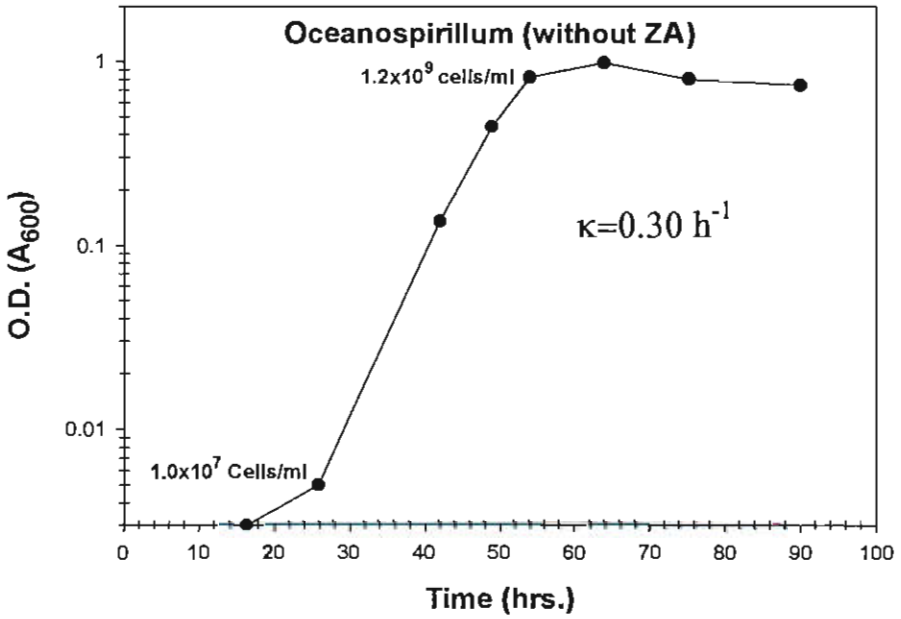
Oceanospirillum (without ZA)
1.2x10^9 cells/ml
κ=0.30 h^-1
1.0x10^7 Cells/ml
O.D. (A600)
1
0.1
0.01
0
10
20
30
40
50
60
70
80
90
100
Time (hrs.)

Fig.8 P. aer (ERC) grwth curves

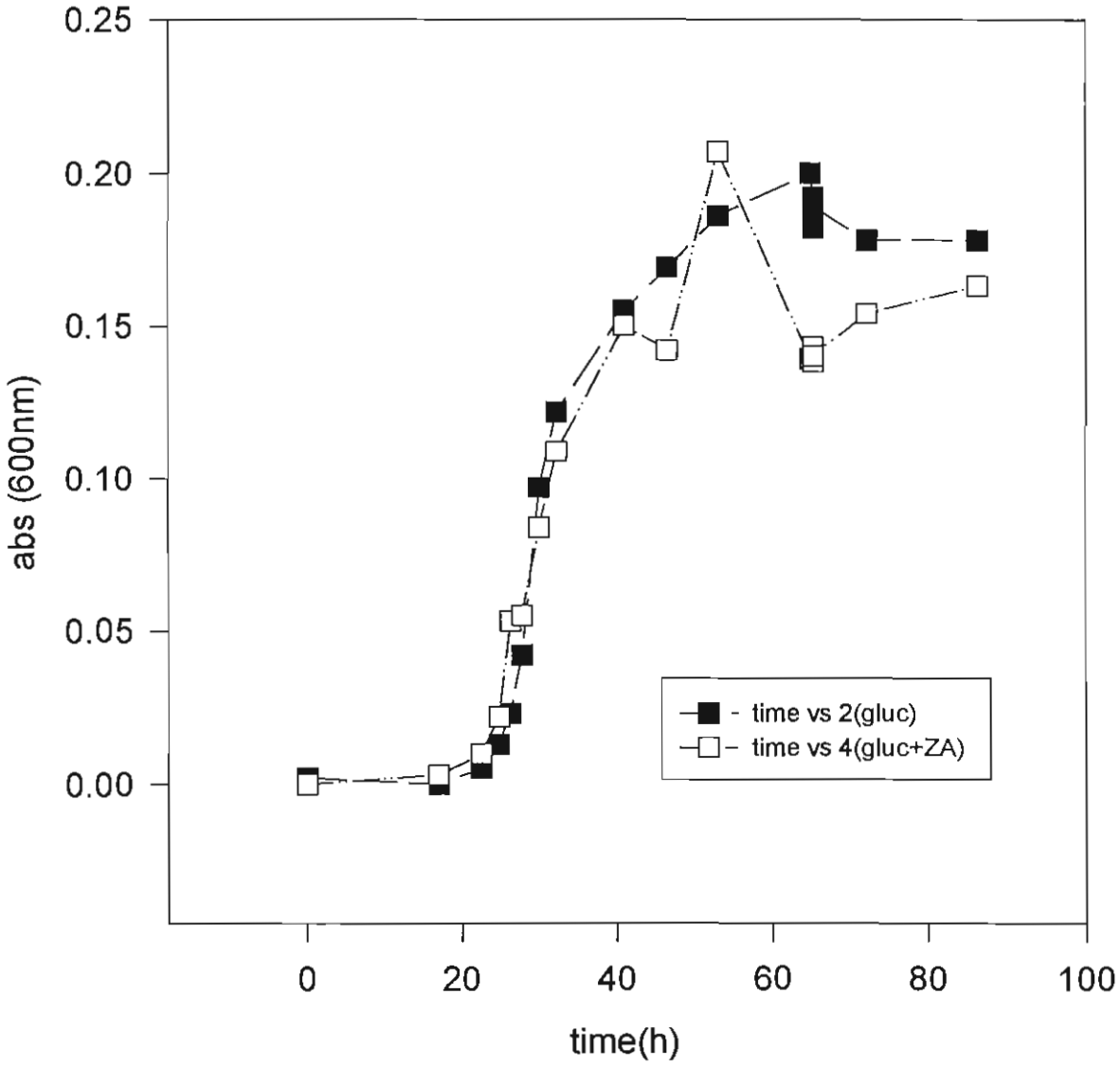

D. Effect of Zosteric Acid on Bacterial Attachment to Cellulose Acetate and Polyamide Reverse Osmosis Membranes

Harry F. Ridgway
Orange County Water District, Fountain Valley, California, 92728-8300

Robert F. Riley
Separation Systems Technology, Inc. 4901 Morena Bl. Bldg. 809, San Diego 92117

1. Bacterial Attachment to Surface-Modified PA Membranes

Two series of surface-modified aromatic cross-linked polyamide (PA) membranes incorporating zosteric acid (ZA) were prepared by Robert L. Riley and colleagues at Separation Systems Technology, San Diego, California. The membrane series included (1) the free-sulfonate (FS) series and (2) the free-carboxyl (FC) series (Figures 1-2). In the FS membrane series, the carboxyl group of the ZA molecule was covalently bonded (via a hydrazine amide linkage) to free carboxyl groups at the PA membrane surface. Thus, the ZA sulfonate group was oriented toward the aqueous phase (Figure 1). In the FC membrane series, ZA was bonded to the membrane carboxyl groups via a sulfonate-amine ionic linkage with the ZA carboxyl group oriented towards the aqueous phase (Figure 2). The preparation and ATR/FT-IR characterization of these surface modified PA membranes is described in greater detail in Section 2.0 of this summary report.

The attachment behavior of *Mycobacterium* strain BT12-100 to the above surface-modified membranes was evaluated using a 'disk assay' procedure outlined in Figure 3. In this laboratory bioassay, mycobacteria uniformly radiolabeled with [^{35}S]sulfate are allowed to come into intimate contact with a disk shaped coupon (about 1 inch in diameter) of the experimental membrane for a specified time period, typically 5 hours at room temperature (shaking at 200 rpm). After incubation, the unattached and loosely attached cells are rinsed off the membrane surface and the firmly adsorbed bacteria are then enumerated by liquid scintillation counting (LSC). Enumeration of radiolabeled bacteria by epifluorescence microscopy allows calculation of cell specific activity and conversion of LSC data to actual bound cells per unit area of membrane surface.

Results from the disk assay method described above are presented in Figures 1-2 for the ZA-modified PA membranes. The data indicate that bacterial attachment was promoted (above that of the unmodified PA membrane control) when the ZA molecule was oriented at the PA membrane surface with the sulfonate group facing outward (FS series). When the ZA molecule was oriented with the carboxyl group facing outward, there was no apparent stimulation of bacterial attachment relative to the unmodified PA membrane control. These data are consistent with (but do not prove) the hypothesis that there is some specificity of the ZA sulfonate group for the bacterial surface and that no such specificity exists for the carboxyl group (see Figure 4).

Effect of Soluble ZA on Bacterial Attachment

Additional bacterial attachment assays were performed in which ZA was added directly to cell suspensions to determine if it would interfere with or otherwise influence cell attachment to unmodified CA and PA membranes in the disk assay procedure. When ZA was added at a concentration of 0.1wt% to a bacterial suspension containing about 1 x 10^8 cells/mL, there was little or no effect on bacterial attachment to CA membrane for both the hydrophobic *Mycobacterium* strain BT12-100 and the hydrophilic *Flavobacterium* strain PA-6 (see Figures 5-6). In contrast, both of these organisms exhibited slightly enhanced attachment to the PA membrane surface compared to untreated control preparations Figures 5-6).

Bacterial attachment studies were also conducted under dynamic flow conditions using a special flow cell that could be directly mounted on the microscope stage, as shown in Figure 7. Using the microscope flow cell (MFC), it was demonstrated that detachment of *Mycobacterium* strain BT12-100 cells from a nascent (48 hr) biofilm formed on CA-coated glass failed to occur when the ZA concentration was varied from 0 to about 0.09wt% in a linear gradient (Figure 8). Pretreatment of the CA membrane surface for about 2 hours with 0.1wt% ZA prior to the introduction of mycobacteria resulted in a noticeable stimulation of cell attachment compared to the untreated control membrane (Figure 9). ATR/FT-IR data presented in Section 2.0 indicated that some ZA remained bound to the CA membrane surface following pretreatment, especially at lower pH values. The attachment of both *Flavobacterium* strain PA-6 and *Mycobacterium* strain BT12-100 to CA membrane was similarly enhanced when 0.05wt% soluble ZA was added concomitantly with cells to the influent to the MFC (Figures 10-11).

In summary, no strong effects of ZA on the inhibition of attachment or detachment of two different bacterial strains (one hydrophobic and one hydrophilic) was observed in this study. However, slight but consistent stimulation of cell attachment was apparent when ZA was used to pretreat CA membranes prior to cell addition, or when ZA was added concomitantly with cells to the MFC influent stream. The stimulation of cell attachment appeared to be independent of the nature of the bacterial cell surface, since it was observed for both a hydrophobic *Mycobacterium* strain and for a hydrophilic *Flavobacterium* strain. The data are consistent with (but do not prove) a model in which ZA is possibly acting as a bridging (cohesive) agent between the bacterial cell surface and the CA or PA membrane surface. However, based on cell attachment data obtained using the surface-modified PA membranes prepared by R. L. Riley and co-workers, it would appear that there is some specificity of interaction between the sulfonate group of ZA and the bacterial cell surface.

2. ZA Surface Modification of PA Membranes and ATR-FTIR Characterization

Methods and Materials

Chemical Attachment of ZA to a PA Composite Membranes. Experimental PA membranes were synthesized with ZA chemically incorporated into surface structure. These membranes were synthesized by R. L. Riley and colleagues at Separations Systems Technology (SST) in San Diego. The ZA was chemically attached to the surface of a standard polyamide FT-30 composite membrane. Two different chemistries were investigated (1) attachment of the

sulfonic acid group to the PA membrane leaving the carboxylic acid group free, and (2) attachment of the carboxylate group to the membrane surface leaving the sulfonic acid group free.

Attachment Sulfonic Acid Group to PA Membrane. Polyamide FT-30 RO composite membranes were prepared by forming a thin PA film on the porous surface of a polysulfone supporting membrane by an *in-situ* interfacial polycondensation reaction between a di-functional amine (*meta*-phenylenediamine; MPD) and a tri-functional acid chloride (trimesolylchloride; TMC) (Figure 12). Initially, the surface of the porous supporting membrane was coated with an aqueous solution of MPD that was adsorbed on the porous membrane surface (Step 1). Subsequently, the aqueous amine coated surface was washed with a hexane solution of TMC (Step 2). At the immiscible interface between the aqueous and the hexane phase, the amine reacts with the acid chloride to form a PA thin film. Upon completion of the PA film, the surface in contact with the hydrocarbon acid chloride phase contains a substantial concentration of pendent acid chloride qroups, which are hiqhly reactive. This surface was washed with hexane (Step 3) to remove all excess TMC, leaving free only those acid chlorides covalently attached to the PA film. An aqueous hydrazine solution was passed over the surface of the PA film and allowed to react with the pendent acid chlorides (Step 4). After this reaction is complete, the surface is washed with water to remove all unreacted hydrazine (Step 5) leaving only free amine groups. Immediately following, the amine groups were protonated by acid washing the surface with a 2.275% solution of HCl (pH 1.5) and then finally washed with a 1.0wt% aqueous solution of ZA (Step 5). The sulfonic acid group of ZA reacts with the protonated amine ($-NH_3^+$) on the surface of the PA film to complete the attachment. In this configuration, the carboxylic acid group of ZA is free on the surface of the PA membrane.

Attachment of the Carboxylate Group to PA Membrane. The ZA was attached to the surface of a PA membrane via the carboxylic acid group to determine if the pendent sulfonic acid group was effective in reducing or otherwise influencing bacterial attachment. The overall procedure, shown in Figure 13, was similar to the one used to attach ZA to the PA membrane surface via the sulfonic acid group. The only difference occurred at Step 2 where the membrane was only washed with water to keep the pendant hydrazine in the amine ($-NH_2$) form; the amine was not protonated by an acid wash. In this way, the amine group was free to react with 1wt% ZA via the carboxylic acid group.

CA Thin Film Cast on Internal Reflection Element. Parallelepiped zinc selenide (50 x 10 x 3 mm) internal reflection elements (IREs) were purchased from Harrick Scientific (Ossining, NY). IREs were washed with detergent, rinsed with tap water, rinsed with 18 Mohm-cm deionized water (E-pure, Barnstead/ Thermolyne, Dubuque, IA) and allowed to air dry. CA (100,000 MW) with varying levels of acetylation was obtained from SST. CA with 43.9% acetylation was dissolved in high purity dichloromethane (B&JGC[2], Burdick & Jackson, Muskegon, MI). Solutions were mixed with a Teflon® stir bar and sonnicated in a warm water bath until the CA was completely dissolved. Solutions were filtered through lens paper to remove insoluble fibrous material.

Thin films of CA were dip-cast onto the IREs using a Pyrex cylinder (20 x 6 cm O.D.) device for the coating process as shown in Figure 14. Compressed air passed through a dryer

(Balston Model 75-20) and a 0.2 μm polytetrafluoroethylene filter was used to purge the cylinder of water vapor. The CA solution (0.5% wt/vol) was mixed with a Teflon® stir bar. The stirring and air purge were turned off prior to casting of the film to eliminate turbulence at the air-solution interface. A peristaltic pump (Masterflex, Cole-Parmer Instrument Co.) was used to withdraw the IRE from the polymer solution. Nylon monofilament (2 lb) was tied to the drive shaft of the pump. IREs were secured to a piece of fine copper wire with Teflon® adhesive tape, and the wire was attached to the nylon line with a small brass fishing swivel. IREs were dipped and then withdrawn from solution at a rate of 1 cm/sec (1.50 pump setting). The flow of air to the cylinder was turned on immediately after the IRE was withdrawn from solution. The ZnSe IREs were dipped once. CA was removed from the end of the IRE with a cotton swab saturated with chloroform. The film thickness was determined by gravimetric analysis. The CA-coated ZnSe IRE was weighed, stripped of CA, dried and then reweighed. The estimated film thickness on the ZnSe IRE dipped once in 0.5% CA solution was 1500 Å.

Attenuated Total Reflectance Fourier Transform Infrared (ATR-FTIR) Spectrometry. Experimental PA membranes with ZA chemically attached to the polymer surface were obtained from SST. Membranes were analyzed by ATR/FT-IR spectrometry. Small strips or swatches of membrane (~ 40 x 10 mm) were cut and pressed against each side of a ZnSe IRE (50 x 10 x 2 mm) using an internal reflection plate holder (Harrick Scientific, Ossining, NY). The plate holder was placed on a twin parallel-mirror reflection attachment (Harrick Scientific) installed in the sample compartment of a Nicolet Magna 550 FT-IR spectrometer (Nicolet Instrument Corp., Madison, WI). The spectrometer was equipped with a medium-range mercury-cadmium-telluride detector (Figure 15). Each spectrum consisted of 256 scans collected at 4-cm^{-1} resolution. Sample spectra were processed using GRAMS/32 software (Version 5.05, Galactic Industries Corp., Salem, NH). The absorbance spectra were corrected to account for the wavelength dependence of ATR measurements of bulk samples.

ZA Adsorption onto CA Thin Films. CA-coated ZnSe IREs were placed in a stainless steel multi-reflection edge-seal liquid cell (Harrick Scientific) (Figure 15). BUNA O-rings formed the seal. Both sides of the IRE were exposed to the aqueous test solutions. The flow cell (1 mL vol) was placed on a twin parallel-mirror reflection attachment (Harrick Scientific) installed in the sample compartment of the spectrometer. Deionized water or aqueous organic test solution (0.5% wt/vol) was pumped through the flow cell at 8 ml/hr. Solutions were not recirculated. Infrared (IR) spectra were collected periodically by a macro program (OMNIC Macros\Basic Version 1.20). A total of 80 scans (1-min acquisition time) at 4-cm^{-1} resolution were coadded and stored for spectral processing. Single-beam IR spectra were processed with GRAMS/32 spectroscopic software (Version 4.0, Galactic Industries, Salem, NH). Macromolecule adsorption on CA was monitored by digitally subtracting a hydrated CA reference spectrum from the sample absorbance spectrum, revealing the underlying spectrum of the adsorbed chemical species. No correction for the wavelength dependence of ATR measurement were made since the adsorbed organic film was less than the depth of penetration of the evanescent wave.

ZA ATR Spectra. Aqueous solutions of ZA were made at a concentration of 1.0wt% in E-pure water. The pH was adjusted with HCl or NaOH. A 50 x 10 x 2 mm Ge IRE was installed in the ATR flow cell. A series of 256 scans were collected at 4 cm^{-1} resolution and coadded. A

water reference spectrum of appropriate pH was digitally subtracted from the each sample to reveal the underlying spectrum of ZA.

Results and Discussion

Aqueous ATR/FT-IR Spectra of ZA. Aqueous mid-infrared ATR reference spectra of **ZA** were collected. The pH was varied from 4 to 10 using HCl or NaOH. Infrared spectra at pH 4, 7 and 10 are shown in Figure **16**. The assignments for some of the major vibrational bands include the antisymmetric and symmetric carboxylate (COO^-) stretch at 1641 cm^{-1} and 1386 cm^{-1}, the antisymmetric and symmetric S=O stretch near 1246 cm^{-1} and 1049 cm^{-1} and the 'semicircle' stretch of para-substituted benzene at 1505 cm^{-1}. As the pH was increased from 4 to 10, a greater portion of the carboxylic acid exists in the deprotonated form. Thus, the magnitudes of the antisymmetric and symmetric stretching bands of the carboxylate group increased with increasing pH.

Chemical Incorporation of ZA on the Surface of a Thin Film PA Membrane: Free Carboxylate Group. A modified PA RO membrane was synthesized with ZA incorporated on the surface. After a six step process (see Figure 12, above), the sulfate ester group of ZA was left ionically bound to the PA membrane with the carboxylic acid left free. The seawater RO performance of the HR-166, HR-167 and HR-168 membranes from steps 4, 5, and 6 was quite good (see Table 1). HR-166 from step 4 had a free amine group, HR-167 from step 5 a protonated amine group and HR-168 zosteric acid ionically bound to the membrane surface with the free carboxylate group. The nature of the active group on the surface of the polyamide membrane had little effect on the reverse osmosis performance.

Table 1

RO Performance of ZA-Modified
PA Composite Membranes

Test Conditions: 800 psi applied pressure, 35,000 mg/mL, NaCl feed, 31°C, pH 6.8

Membrane Designation	Synthesis Step (Figure x.x)	Surface Active Group	Water Flux (gfd)	Rejection (%)
HR-166	Step 4	$-NH_2$	16.8	96.8
HR-167	Step 5	$-NH_3^+$	17.6	95.3
HR-168	Step 6	PA-ZA[COOH]	17.1	95.8

Free Sulfate Ester Group. A second modified PA membrane was synthesized. ZA was covalently bound to the surface the PA membrane via the carboxylic acid group. The six step

synthesis is shown in Figure 13 (above) and was similar to the one used to generate the HR-160 series of PA membranes. The only difference occurred at Step 2 where the PA membrane was washed with water (instead of acid) to keep the pendant hydrazine in the amine form. In this way, the amine ($-NH_2$) was free to react with the carboxylic acid group of ZA.

The seawater RO performance of the membranes HR-173 from Step 4, HR-174 from Step 5 and HR-175 from Step 6 are shown in Table 2. Again, no significant difference in transport properties was observed with these membranes.

Table 2

RO Performance of ZA-Modified
PA Composite Membranes

Test Conditions: 800 psi applied pressure, 35,000 mg/L, NaCl feed, 31°C, pH 6.8

Membrane Designation	Synthesis Step (Figure x.x)	Surface Active Group	Water Flux (gfd)	Rejection (%)
HR-173	Step 4	$-NH_2$	15.3	95.1
HR-174	Step 5	$-NH_2$	18.0	96.1
HR-175	Step 6	PA-ZA[$SO3^-$]	19.5	95.9

ATR/FT-IR Spectra of ZA-Modified PA Membranes: Free Sulfate Ester ($-OSO_3^-$) Group. ATR/FT-IR spectra were collected to verify the presence of the ZA adduct. Small swatches of membrane were pressed against the surface of a ZnSe IRE. ATR/FT-IR spectra of membranes HR-173, HR-174 and HR-175 between 4000 and 600 cm^{-1} are displayed in Figure 17. Spectra of the three HR membranes, a reference spectrum of a standard PA (FT-30) membrane and an aqueous transmission spectrum of ZA are displayed (2000 and 600 cm^{-1}) in Figure 18. Based on the proposed reaction scheme, membranes HR-173 and HR-174 should both possess a free amine ($-NH_2$) (see Figure 13 [reaction scheme] and Figure 18 [spectra]). Therefore, antisymmetric and symmetric $-NH_2$ stretching bands between 3398 – 3381 cm^{-1} and 3340 – 3324 cm^{-1} should be visible in the IR spectra. Overlapping bands are visible in this region, although they are rather weak (Figure 19). The HR-175 membrane was synthesized to have a free sulfate ester group (Figure 13); however, there is no strong indication ZA is covalently bound to the membrane surface. The presence of the antisymmetric and symmetric S=O stretching bands in the HR-175 membrane spectrum is lacking. All three HR membrane spectra look very similar. The HR PA-based membranes differ from the standard PA FT-30 membrane in several ways. The broad O-H stretching band near 3317 cm^{-1} in the PA spectrum was not detected in any of the HR spectra. A broad feature center near 1200 cm^{-1} in the HR spectra is not visible in the standard PA spectrum. While a broad feature in the standard PA spectrum near 1050 cm^{-1} is not visible in the HR-170 series of spectra. Results from IR spectra of the HR-170 series of membranes suggest that the surface modification was unsuccessful or occurred at too low of a yield to detect by the ATR/FT-IR contact method. More work needs to be done to validate where the chemical synthesis was successful. The stability of the hydrazine structures of HR-173 and HR-174 is questionable.

Free Carboxylate Group. ATR/FT-IR spectra of the HR-160 series of membranes were

collected to verify the chemical synthesis and the presence of ZA bound to the membrane surface. Small swatches of membrane were pressed against the surface of a ZnSe IRE. IR spectra (4000—600 cm^{-1}) of membranes HR-166, HR-167, HR-168 and standard PA are shown in Figure 20. Membrane HR-166 should possess a free amine ($-NH_2$), membrane HR-167 should exist as a protonated amine ($-NH_3^+$), and membrane HR-168 should have ZA ionically bound to it, based on the proposed reaction scheme (see Figure 12 [reaction scheme] and Figure 20 [spectra]). N-H stretching bands are visible at 3304 cm^{-1} and 3250 cm^{-1} in the spectrum of HR-167, which suggest the presence of the primary amine salt ($-NH_3^+$) (Figure 21). These two bands virtually disappear following the final rinse with ZA (Step 6, HR-168). It is questionable as to whether the amine salt ($-NH_3^+$) exists following the acid rinse (Step 5, HR-167). The HR-160 series of spectra, the standard PA (FT-30) membrane and an aqueous transmission spectrum of ZA are displayed (2000 and 600 cm^{-1}) in Figure 22. The three HR membranes are similar; however, there are some differences worth noting. The greatest difference is visible in the HR-167, the membrane treated with the acid rinse forming the primary amine salt ($-NH_3^+$). There is a doublet near 1200 cm^{-1} and another double near 950 cm^{-1}. These are best revealed by digitally subtracting the HR-168 spectrum from the HR-167 spectrum (Figure 23). These two doublets were lost after the membrane was treated with the aqueous solution of ZA (Step 6). A negative band appeared near 1050 cm^{-1} (S=O), possibly indicating that some ZA was adsorbed on the HR-168 membrane. Whether it absorbed according to the chemistry described is difficult to determine. Again, more work needs to be done to verify the chemistry used to create these membranes.

Adsorption of ZA on CA Thin Film Determined by ATR/FT-IR Spectrometry. A 0.1wt% solution of ZA was pumped through a flow cell containing a CA(43.9% acetyl)-coated ZnSe IRE. After 4 hr the thin film was rinsed with MS buffer (pH7) to the end of an 8-hr experiment. Infrared spectra of ZA adsorbed on CA were revealed by generating difference spectra, where a hydrated CA reference was digitally subtracted from each sample spectrum. Two ATR spectra (T = 4 hr and T = 8 hr) of ZA adsorbed on a CA thin film are shown in Figure 24. There are weak bands located near 1090, 1018 and 990 cm^{-1} that are similar to those in the ZA reference spectrum. The presence of the most intense vibrational band of ZA, the 1049 cm^{-1} S=O stretch, is questionable. The data can be interpreted in two ways: (1) the 1049 cm^{-1} band of ZA shifted slightly to higher wavenumber upon adsorption to CA or the 1049 cm^{-1} C-O backbone stretch from CA thin film shifted to higher wavenumber. The latter is probably true. That the 1049 cm^{-1} band is derivative in shape is further indication that the C-O band shifted. However, we still would like to believe that some ZA adsorbed on the CA film and remained bound throughout the 4-hr rinse in spite of the low signal-to-noise ratio of the spectra.

The experiment was run again, but the pH was dropped to 4 to shift the ZA equilibrium toward the acid form. As described above difference spectra were obtained by subtracting a hydrated CA reference spectrum from each sample spectrum. The new spectra were more complex than those observed at pH 7 (Figure 25) and more features of ZA were visible. The 1049 cm^{-1} S=O band, 1641 cm^{-1} antisymmetric carboxylate and 1545 cm^{-1} bands were all visible. However, these bands are superimposed on the broad 1049 cm^{-1} C-O stretching band of CA and the 1640 cm^{-1} water band that were not completely subtracted from the sample spectrum. The region around the 1508 cm^{-1}, the semicircle ring stretch, proved to be the vibrational band to monitor ZA adsorption on the CA thin film, as very little interference from the IR spectrum of CA was observed (Figure 25). The IR difference spectra of ZA on CA collected during the 8-hr experiment are displayed in Figure 26. Also shown is a plot of the 1508 cm^{-1} band intensity as a

function of time of flow. A band intensity of 11 mAU was measured within the first minute of exposure representing adsorbed and bulk ZA. An MS buffer rinse was initiated at T = 4 hr. The 1508 cm^{-1} band intensity continued to increase during the buffer rinse even though flow of ZA to the flow cell was stopped. The data does not appear to be random in nature, which leads one to rule out experimental error. These results suggest that the benzene ring became positioned closer to the surface of the IRE where the electric field is greater (E_o) is greater. ZA may have penetrated into the pore structure of CA during the buffer rinse. Molecular rearrangement could occur at the interface as the bulk phase is flushed from the flow cell and replaced by buffer.

Changes in the CA spectrum indicate that ZA adsorbed to the surface of the thin film. When the CA was initially hydrated, the carbonyl band shifted to lower wavenumber, moving from 1749 cm^{-1} to 1747 cm^{-1}. The C-O-C acetate ester band shifted to higher wavenumber, moving from 1230 cm^{-1} to 1232 cm^{-1}. Similar shifts in frequency have been reported by Toprak and coworkers.[i] These frequency shifts occur when hydrogen bonds form with the carbonyl and acetate ester groups on CA. Upon exposure to 0.5% ZA, the carbonyl band of CA shifted back to higher wavenumber and the C-O-C acetate ester back to lower wavenumber. These shifts are evident by the derivative bands that form near 1743 cm^{-1} and 1248 cm^{-1} when the hydrated CA reference spectrum was subtracted from the sample spectrum (Figure 27). These shifts indicate displacement of water from the CA interface and loss of hydrogen bonding with the CA thin film.

3. Summary.

Experimental membranes with zosteric acid chemically incorporated on the surface of a standard polyamide FT-30 thin film composite membrane were analyzed by ATR/FT-IR spectrometry. Analysis of the infrared ATR spectra suggest at some of the chemistry may not have occurred as outlined in the procedures. Insufficient sensitivity for the detection of very low concentrations of bond and adsorbed chemical species make interpretation of data difficult. While some ZA appears to be attached to the HR-168, it is not clear whether ZA is ionically bound to a primary amine ($-NH_3^+$) as envisioned in the protocol. More work needs to be done to validate the products from each step of the proposed the reaction scheme.

At pH 7 ZA adsorption on a thin film of cellulose acetate (43.9% acetyl) was difficult to detect. While the ZA concentration was relatively low, 0.1wt%, detection of adsorbed other macromolecules at similar concentration have been detected.[ii] Zosteric acid has a net negative charge at pH 7. CA also has a slight negative charge at this pH.[iii,iv] Therefore, electrostatic repulsion between the thin film and the organic macromolecule may lead to reduced adsorption at the aqueous-polymer interface. When the pH was dropped to 4, a greater amount of ZA was detected at the aqueous-polymer interface. Presumably electrostatic charge repulsion was reduced, and hydrogen bonding between the carboxylic acid on zosteric acid and cellulose acetate increased. Water flux and salt rejection were not affected significantly when a standard cellulose acetate and polyamide FT-30 membrane were operated on a 100 ppm (0.01%) feed of ZA for 6 to 11 hr.[v] Zosteric acid's apparent low affinity for the membrane surface may serve as an explanation for these results. Similar studies with a 0.01wt% solution of benzalkonium chloride resulted in an irreversible loss (-23%) of water flux.[vi]

These studies were part of a larger project devoted to the assessment of ZA use in water treatment systems. For more information see National Water Research Institute Project entitled, "Biofouling Control Through Non-Toxic Means: Application of ZA to Water Treatment Systems. A Phase I Research Program." Project No. TT 699-547-97.

4. References

Toprak, C., J. N. Agar and M. Falk. 1979. State of water in cellulose acetate membranes. J. Chem. Soc. Faraday I **75**:803-815.

Ishida, K. P., R. M. Bold and H. R. Ridgway. 1998. Influence of molecular conditioning films on microbial colonization of synthetic membranes determined by internal reflection spectrometry. Final Report. National Water Research Institute Project No. MRDP 699-508-95.

Childress, A. E., M. Elimelech. 1996. Effect of solution chemistry on the surface charge of polymeric reverse osmosis and nanofiltration membranes. J. Membrane Sci. **119**:253-268.

Dimisch, H.-U. and W. Pusch. 1979. Electric and electrokinetic transport properties of homogeneous weak ion exchange membranes. J. Colloid Interface Sci. **69**:247- .

Lin, S., C. L. Milstead, J. Muira, R. L. Riley and H. H. Ridgway. "Biofouling Control Through Non-Toxic Means: Application of Zosteric Acid to Water Treatment Systems. A Phase I Research Program." NWRI Project No. TT 699-547-97 Progress Report. June 1 to August 30, 1997.

Riley, R. L., C. L. Milstead, J. Safarik, K. P. Ishida and H. R. Ridgway. Unpublished data.